Published in Palaeogeography, Palaeoclimatology, Palaeoecology 2754 : 1-32, 2002,
which should be used for any reference to this work

Late Cretaceous to early Paleocene climate and sea-level fluctuations: the Tunisian record

Thierry Adatte [a,*], Gerta Keller [b], Wolfgang Stinnesbeck [c]

[a] *Institut de Géologie, 11 Rue Emile Argand, 2007 Neuchatel, Switzerland*
[b] *Department of Geosciences, Princeton University, Princeton, NJ 08544, USA*
[c] *Geologisches Institut, Universitat Karlsruhe, 76128 Karlsruhe, Germany*

Abstract

Climate and sea-level fluctuations across the Cretaceous–Tertiary (K–T) transition in Tunisia were examined based on bulk rock and clay mineralogies, biostratigraphy and lithology in five sections (El Melah, El Kef, Elles, Ain Settara and Seldja) spanning from open marine to shallow inner neritic environments. Late Campanian to early Danian trends examined at El Kef and Elles indicate an increasingly more humid climate associated with sea-level fluctuations and increased detrital influx that culminates at the K–T transition. This long-term trend in increasing humidity and runoff in the Tethys region is associated with middle and high latitude cooling. Results of short-term changes across the K–T transition indicate a sea-level lowstand in the latest Maastrichtian about 25–100 ka below the K–T boundary with the regression marked by increased detrital influx at El Kef and Elles and a short hiatus at Ain Settara. A rising sea-level at the end of the Maastrichtian is expressed at Elles and El Kef by deposition of a foraminiferal packstone. A flooding surface and condensed sedimentation mark the K–T boundary clay which is rich in terrestrial organic matter. The P0–P1a transition is marked by a sea-level lowstand corresponding to a short hiatus at Ain Settara where most of P0 is missing and a period of non-deposition and erosion in the lower part of P1a (64.95 Ma). At Seldja, P0 and possibly the topmost part of CF1 are missing. These sea-level fluctuations are associated with maximum humidity. These data suggest that in Tunisia, long-term environmental stresses during the last 500 ka before the K–T boundary and continuing into the early Danian are primarily related to climate and sea-level fluctuations. Within this long-term climatic trend the pronounced warm and humid event within the latest Maastrichtian Zone CF1 may be linked to greenhouse conditions induced by Deccan volcanism. The absence of any significant clay mineral variations at or near the K–T boundary and Ir anomaly suggests that the bolide impact had a relatively incidental short-term effect on climate in the Tethys region.

Keywords: sea-level; climate fluctuations; K–T boundary; Upper Campanian; Maastrichtian; Tunisia; bulk; clay minerals; organic matter; geochemistry

1. Introduction

There are relatively few studies that detail long-term climate and sea-level changes during the late Cretaceous which was generally assumed to have

* Corresponding author. Tel.: +41-32-718-26-18; Fax: +41-32-718-26-01.
E-mail address: thierry.adatte@geol.unine.ch (T. Adatte).

been equally warm. Recent stable isotope studies, however, have revealed that the Maastrichtian global climate was significantly cooler than during the earlier Cretaceous. Strong climate and temperature fluctuations mark the late Campanian and Maastrichtian, as indicated from stable isotope records from the equatorial Pacific (Site 463, Keller and Li, in press) and middle and high latitude South Atlantic (Sites 525, 689 and 690, Barrera and Huber, 1990; Barrera, 1994; Barrera et al., 1997; Li and Keller, 1998a,b). The first major global cooling occurred between 71 and 73 Ma and decreased intermediate water temperatures by 5–6°C and surface temperatures by 4–5°C in middle and high latitudes. Between 68.5 and 70 Ma, intermediate waters warmed by 2°C. Global cooling resumed between 68.5 and 65.5 Ma when intermediate water temperatures decreased by 3–4°C and sea surface temperatures decreased by 5°C in middle latitudes. About 450–200 ka before the Cretaceous–Tertiary (K–T) boundary rapid global warming increased intermediate and sea surface temperatures by 3–4°C, though sea surface temperatures changed little in low latitudes (Li and Keller, 1998b). Beginning about 200 ka before the end of the Maastrichtian, climate cooled rapidly by 2–3°C in both surface and intermediate waters and warmed again during the last 50–100 ka of the Maastrichtian (Li and Keller, 1998b; Stueben et al., this volume).

These global climatic changes were associated with major sea-level fluctuations as expressed in a variety of sea-level proxies, including bulk rock and clay mineral compositions, stable isotopes, total organic carbon (TOC), Sr/Ca ratios and macro- and microfaunal associations. Based on these sea-level and climate proxies, Li et al. (1999, 2000) have identified seven major sea-level regressions during the last 10 myr of the Cretaceous at El Kef and Elles (Tunisia): late Campanian (~74.2 Ma, 73.4–72.5 Ma and 72.2–71.7 Ma), early Maastrichtian (70.7–70.3 Ma, 69.6–69.3 Ma and 68.9–68.3 Ma), and late Maastrichtian (65.45–65.50 Ma). Low sea-levels are generally associated with increased terrigenous influx, low kaolinite/chlorite+illite ratios, high TOC and high Sr/Ca ratios, whereas high sea-levels are generally associated with the reverse conditions. In addition, climatic changes inferred from clay mineral contents correlate with sea-level changes. Warm or humid climates accompany high sea-levels and cooler or arid climates generally accompany low sea-level (Li et al., 2000).

The global sea-level fluctuations are linked to climatic changes (Li et al., 1999) and inversely correlate with species diversity in planktic foraminifera (e.g. diversity maximum follows maximum cooling at 70.7–70.3 Ma; diversity decline follows warming at 65.4–65.2 Ma, Li and Keller, 1998a,c). But precisely how climate changed across the K–T boundary mass extinction and during the subsequent evolution of early Tertiary faunas is still an enigma largely because diagenetic alteration of carbonates obscures the oxygen isotope records (see Stueben et al., this volume).

A number of studies have attempted to reconstruct the sea-level history across the K–T transition in Tunisia based on benthic and planktic foraminifera, dinoflagellates or palynofloras (e.g. Brinkhuis and Zachariasse, 1988; Keller, 1988b, 1992; MacLeod and Keller, 199la,b; Schmitz et al., 1992; Speijer, 1994; Keller and Stinnesbeck, 1996; Brinkhuis and Visscher, 1994; Brinkhuis et al., 1998; Galeotti and Coccioni, 2002). The overall sea-level trends in these studies are in general agreement, though may vary in the details and the timing of sea-level lowstands. A major problem has been the absence of oxygen isotope-inferred climate data to support sea-level fluctuations inferred from faunal and floral proxies. Oxygen isotope data are frequently not reliable temperature indicators across the K–T transition because of diagenetic alteration of carbonate and recrystallization of foraminiferal tests (Oberhaensli et al., 1998; Stueben et al., this volume). Alternate temperature proxies based on the coiling direction of the benthic foraminifera *Cibicidoides pseudoacutus* (Galeotti and Coccioni, 2002) and the ratio of warm/cool dinocysts (Brinkhuis et al., 1998) have been proposed, but these have yet to be independently confirmed.

This study evaluates climate and sea-level changes across the K–T transition based on lithological characteristics, bulk rock and clay mineral data from several Tunisian sections that span from upper slope (El Melah) to outer neritic (El

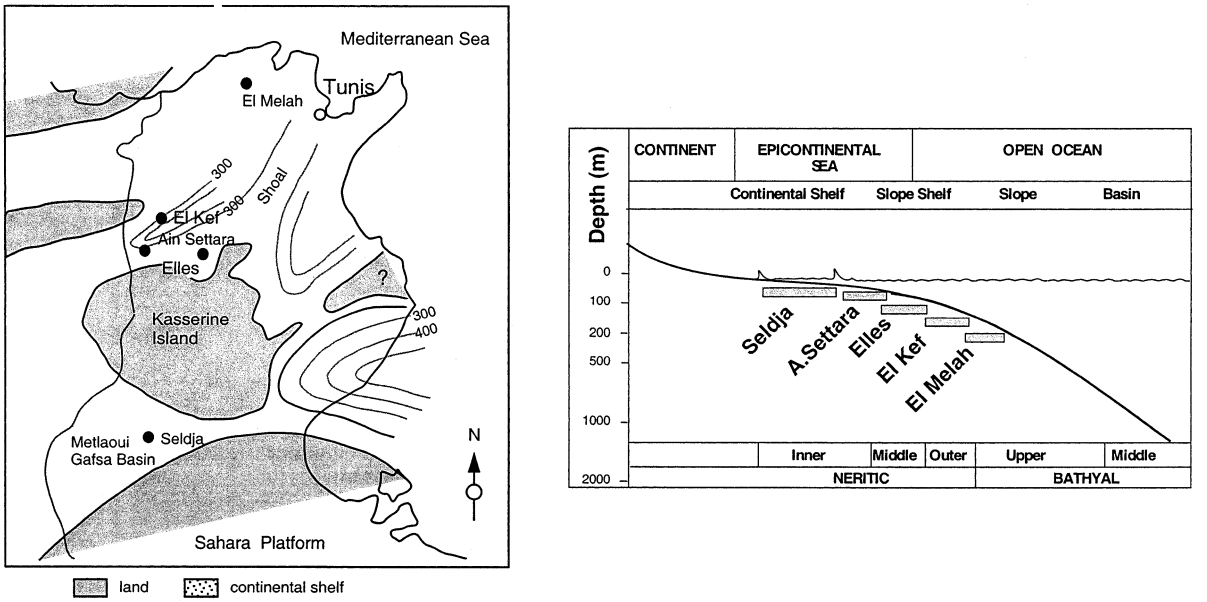

Fig. 1. Paleoenvironmental settings of five Tunisian K–T sections spanning from the restricted shallow Gafsa Basin (Seldja section) at the edge of the Sahara to the middle and outer shelf depths of the El Kef, Elles and Ain Settara sections to the north of the Kasserine Island, and to the upper bathyal El Melah section to the north (modified after Burollet, 1956; Burollet and Oudin, 1980). Isopach lines are given in meter for the Maastrichtian interval.

Kef, Elles), middle neritic (Ain Settara) and inner neritic (Seldja) environments (Fig. 1). The time interval analyzed spans from the uppermost Maastrichtian Zone CF1 to the early Danian Zone Plb or Plc. In addition, we examine long-term trends based on bulk rock and clay mineral data from the late Campanian through Maastrichtian of the Elles and El Kef sections.

2. Methods

In the field, sections were cleaned from surface contamination by digging a trench to fresh bedrock. Samples were then collected at 5–10 cm intervals and at closer 1–2 cm intervals across the K–T boundary clay layer. For each section, the same sample set was used for faunal, geochemical and mineralogical studies to insure direct comparison of results (see Keller et al., 2002; Stueben et al., this volume). Biostratigraphy is based on planktic foraminifera and the zonation of Keller et al. (1995) for the K–T transition and of Li and Keller (1998c) for the late Campanian and Maastrichtian of Elles and El Kef sections. Biostratigraphic data for each section are based on published studies: Elles I and El Melah from Karoui-Yakoub et al. (2002), Elles II K–T transition from Keller et al. (2002) and upper Maastrichtian from Abramovich and Keller (2002), Ain Settara from Luciana (2002) and Seldja from Keller et al. (1998). Sediment accumulation rates were calculated based on the time scale of Cande and Kent (1995).

Whole rock and clay mineral analyses were conducted at the Geological Institute of the University of Neuchatel, Switzerland, based on XRD analyses (SCINTAG XRD 2000 Diffractometer). Sample processing followed the procedure outlined by Kübler (1987) and Adatte et al. (1996). XRD analyses of the whole rock were carried out for all the samples at the Geological Institute of the University of Neuchatel. The samples were prepared following the procedure of Kübler (1987). Random powder of the bulk samples is used for characterization of the whole rock mineralogy. Nearly 20 g of each rock sample was ground with a 'jaw' crusher to obtain small rock

chips (1–5 mm). Approximately 5 g was dried at a temperature of 60°C and then ground again to a homogeneous powder with particle sizes < 40 μm. About 800 mg of this powder was pressed (20 bar) in a powder holder covered with a blotting paper and analyzed by XRD. Whole rock composition is based on methods described by Ferrero (1965, 1966), Klug and Alexander (1974) and Kübler (1983). This method for semi-quantitative analysis of the bulk rock mineralogy (obtained by XRD patterns of random powder samples) used external standards with an error varying between 5 and 10% for the phyllosilicates and 5% for grain minerals.

Clay mineral analyses were based on methods by Kübler (1987). Ground chips were mixed with de-ionized water (pH 7–8) and agitated. The carbonate fraction was removed with the addition of HCl 10% (1.25 N) at room temperature for 20 min, or more until all the carbonate was dissolved. Ultrasonic disaggregation was accomplished during 3 min intervals. The insoluble residue was washed and centrifuged (5–6 times) until a neutral suspension was obtained (pH 7–8). Separation of different grain size fractions (< 2 μm and 2–16 μm) was obtained by the timed settling method based on Stokes law. The selected fraction was then pipetted onto a glass plate and air-dried at room temperature. XRD analysis of oriented clay samples was made after air drying at room temperature and ethylene-glycol solvated conditions. The intensities of selected XRD peaks characterizing each clay mineral present in the size fraction (e.g. chlorite, illite, kaolinite, smectite) were measured for a semi-quantitative estimate of the proportion of clay minerals present in the size fractions < 2 μm and 2–16 μm (error $\pm 5\%$). Therefore, clay minerals are given in relative percent abundance without correction factors. Content in swelling (% smectite) is estimated by using the method of Moore and Reynolds (1989). Determination of chlorite and kaolinite is obtained by deconvolution of their 002 and 004 peaks respectively at 24.9° (kaolinite) and 25.2° (chlorite).

Organic carbon analysis was conducted using a CHN Carlo-Erba Elemental Analyzer NA 1108. Total carbon was first measured on bulk samples (0.01–0.02 g). Total organic carbon (TOC) was determined after removing carbonate by acidification with hydrochloric acid (10%), assuming that dissolved organic matter in ancient sediments is nearly absent. The obtained values were compared with a standard reference sample. Analytical precision for a standard is $\pm 0.003\%$ and reproducibility for the Maastrichtian samples is 0.01% for bulk rocks (total carbon) and 0.02% for insoluble residues.

3. Lithology

3.1. El Melah K–T

The El Melah section is located near the village of El Aouana about 150 km northeast of El Kef and 60 km northwest of Tunis (see Karoui-Yakoub et al., 2002 for directions). The El Melah outcrop is 10 m thick and located on the right side of the Oued el Maleyh. The section spans 2 m of the uppermost Maastrichtian Zone CF1 and 8 m of Danian sediments (Fig. 2). The uppermost 5 cm of the Maastrichtian gray marls are highly bioturbated. The K–T boundary is marked by a thin rusty red layer similar to Elles and El Kef. A 20 cm thick dark organic-rich clay of Danian age overlies the red layer and is strongly bioturbated (Fig. 3). The earliest Danian Zone P0 spans the first 10 cm of this dark clay layer, followed by 1.4 m of Zone Pla (Karoui-Yakoub et al., 2002). Gray shales and marls alternate upsection and marls are increasingly more dominant in Zones

Fig. 2. Biostratigraphic correlation of the K–T transition in the five studied sections which span a distance of more than 450 km from the north to the south of Tunisia. Note that Zone P0 is most expanded (50 and 60 cm) at the El Kef and Elles sections, condensed (10 cm) at El Melah, mostly missing at Ain Settara due to a hiatus (only 2 cm present), and absent at Seldja due to a hiatus.

N
S
El Melah
El Kef
Elles I + II
Ain Settara
Seldja
Stages
Depth(m)
Biozones
Lithology
U.Ma.
L. Paleocene
U. Maastr.
CF1
P0
P1a
P1b
P1c
P1d
P2-3
EL I
EL II
marl
marly clay
clayey marl
sandstone
(with mud clasts)
sandstone
(with phosphatic nodules)
TUNIS
El Melah
El Kef
A.Settara
Elles
Kalaat
Senam
Sousse
Kairouan
Sfax
Gabes
KASSERINE
ISLAND
Mellaoul
Safsa
Seldja
Saharan Platform
100 Km
Depth (m)
SELDJA
A.SETTARA
ELLES
EL KEF
EL MEHLA
OPEN OCEAN
EPICONTINENTAL SEA
CONTINENT
Basin
Slope
Slope-Shelf
Continental Shelf
Middle
Upper
Outer
Middle
Inner
NERITIC
BATHYAL

P1a–P1b. Beginning at 7.40 m above the K–T boundary (P1d) marly limestones are interbedded with marls (Fig. 2).

Paleogeographically, El Melah was located in an outer neritic to upper bathyal environment (300–400 m deep in the Tunisian trough about 200 km north of the Kasserine Island (Fig. 1). The El Melah area was thus less influenced by terrigenous influx than sections to the south (Burollet, 1956). Consequently, sediment accumulation rates are lower compared to El Kef and Elles. At El Melah, sediment accumulation rates average 0.35 cm/ka for the P0–P1a interval based on the time scale of Cande and Kent (1995). The comparatively low sediment accumulation rate mainly reflects sediment starvation due to its paleo-location and distance from a terrigenous source.

3.2. El Kef K–T

The El Kef K–T stratotype is located in northwestern Tunisia about 7 km west from the town of El Kef and 75 km from Elles (Fig. 1; see Keller et al., 1995 for precise location). In recent years, the section has been heavily sampled and agricultural encroachment and grazing obscure the outcrop (Remane et al., 1999). The uppermost Maastrichtian consists of 4.5 m of gray marls (CF1) followed by a 3 mm thick rusty red clay layer (Figs. 2, 3). This red layer is between two thin layers of secondary gypsum, goethite and jarosite, similar to Elles and El Melah sections. About 20 cm below the K–T boundary red layer is a 10 cm thick layer which is significantly enriched in foraminifera and correlates with the foraminiferal packstone observed at Elles I and II outcrops (Fig. 3) (Keller et al., 2002). Above the K–T red clay layer is a 60 cm thick dark gray shale layer (Zone P0) which grades upwards into marly shales (Fig. 2, P1a–P1b).

Compared with El Melah, the El Kef section was located closer to the emerged Kasserine Island and in a shallower outer neritic to upper bathyal environment ($\sim$200–300 m, Fig. 1). Sediment deposition occurred in open marine conditions, but with significant terrigenous influx predominantly from the Kasserine Island and intermittent influx from emerged land located to the west of El Kef. Sediment accumulation rates based on the time scale of Cande and Kent (1995) average 2 cm/ka for the latest Maastrichtian Zone CF1 (Li and Keller, 1998a,b,c), about 1.1 cm/ka for Zone P0, and 1.9 cm/ka for Zone Pla.

3.3. Elles I and Elles II K–T

The Elles sections are located in the Karma valley about 75 km southeast of El Kef near the hamlet of Elles (see Karoui-Yakoub et al., 2002 for directions). Campanian through Eocene sediments outcrop along the Karma valley which forks into two parts within late Maastrichtian sediments. The Elles I section was collected in the right valley fork which exposes about 7–8 m of Maastrichtian sediments and about 20 m of Danian sediments (Fig. 2) (see Karoui-Yakoub et al, 2002). Elles II was collected in the left valley fork which exposes about 50 m of Maastrichtian sediments and continues for several hundred meters across the K–T boundary and through the Paleocene.

At Elles I, the latest Maastrichtian is composed of about 7–8 m of gray shales and marls with several resistant marly limestone layers between 4 and 7 m below the K–T boundary. The K–T transition is well marked by a 0.5–1.0 cm clay layer and a 3–4 mm thick rusty red layer embedded between two gypsum-jarosite layers of late diagenetic origin. The red clay layer is overlain by a 60 cm thick dark clayey interval (Zone P0), followed by 5.5 m of gradually lighter shales and shaley marls. Upsection, these sediments are interbedded with marly limestones (P1b). The stratigraphic interval considered in this study includes the uppermost meter of the Maastrichtian (CF1 Zone), the K–T boundary (P0) and the first 7 m of the Danian (P1a–P1b, Figs. 2, 3) biostratigraphy after Karoui-Yakoub et al., 2002).

Elles II differs from Elles I primarily in the more expanded K–T transition and the presence of a 5–10 cm foraminiferal packstone with ripple marks below the K–T boundary clay and red layer (Fig. 3). The uppermost Maastrichtian at Elles II is characterized by a monotonous sequence of dark gray siltstones, silty shales, marls and sandy marls (CF1). A few Fe concretions

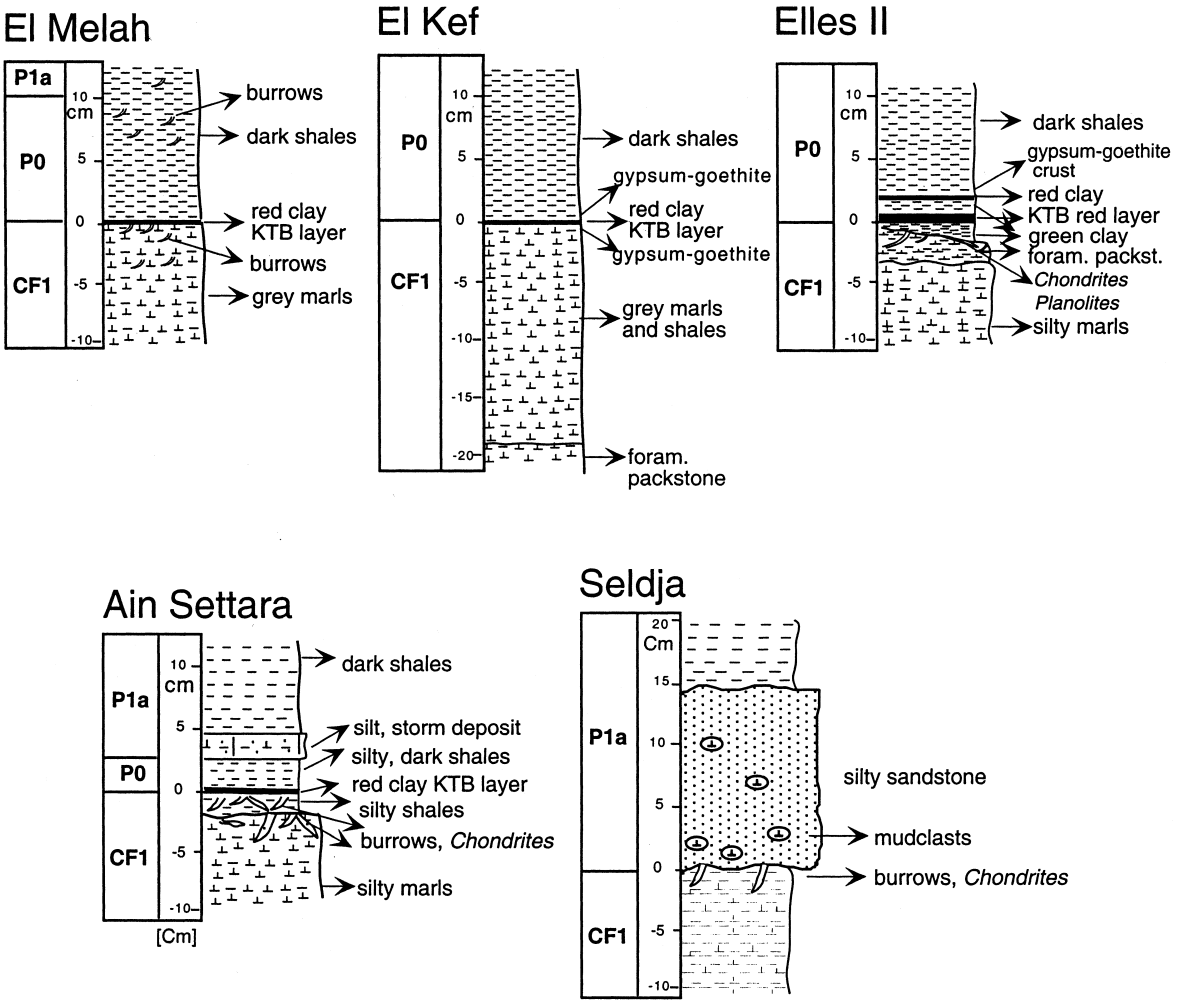

Fig. 3. Expanded stratigraphic interval and lithological characteristics across the K–T transition in the five studied outcrops. With the exception of Seldja, all sections contain the characteristic thin red layer rich in Ir and spinels which marks the K–T boundary mass extinction of tropical and subtropical planktic foraminifera. Dark organic-rich clay overlies the red layer in all sections and marks Zone P0. Gypsum of diagenetic origin is usually present above and below the red layer. At Elles II a second red layer is present. Hiatuses at or near the K–T boundary can be identified by the thin Zone P0 clay layer (Ain Settara) and the truncated burrows (El Melah, Elles II, Ain Settara (two intervals), and Seldja). A foraminiferal packstone is present near the top of the latest Maastrichtian Zone CF1 at El Kef and Elles II and marks a flooding surface, winnowing and condensed sedimentation.

(goethite) up to 1 cm in diameter are also present. Many intervals are mottled due to ichnofaunal activity and individual traces are rarely preserved due to the soft pelitic sediment. In several horizons, however, we determined *Chondrites*, *Planolites* and possibly *Teichichnus*, whereas megafossils appear to be absent.

An important sedimentological change occurs at the top of the sequence. In the 30 cm thick interval directly underlying the K–T boundary, gray marls first grade into gray calcareous siltstones and then into gray calcarenitic marly limestones, both of which form layers of 5 and 8 cm thick respectively. Overlying this interval is a 5–7

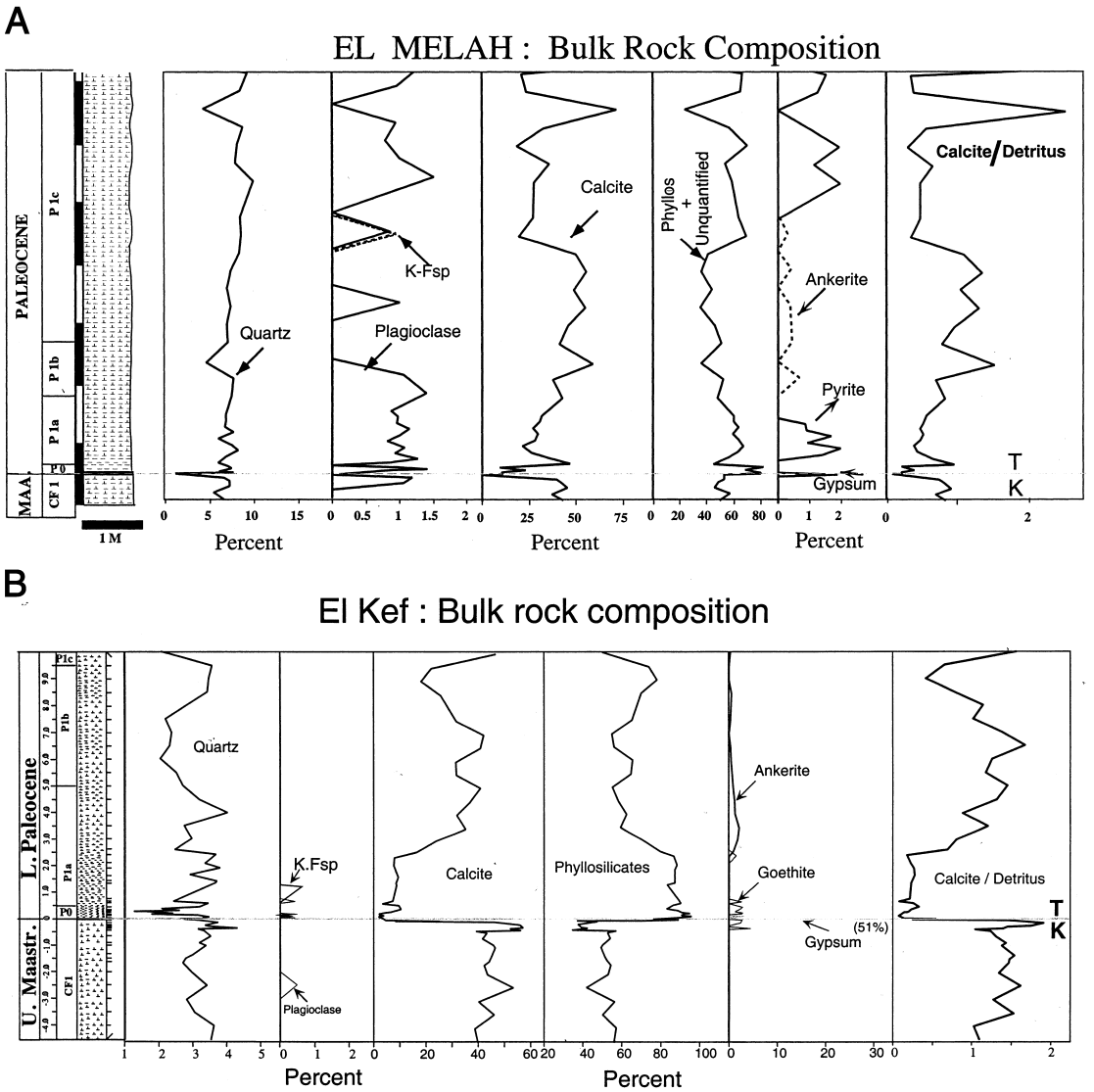

Fig. 4. Bulk rock compositions at (A) El Melah, (B) El Kef, (C) Elles and (D) Seldja. Note that the dominant sedimentary components are phyllosilicates and calcite with temporally restricted influx of quartz, plagioclase and K-feldspar. A major compositional change occurs at the K–T boundary in all sections examined, though no exotic minerals were observed at this interval.

cm thick yellow calcarenitic marly limestone consisting primarily of planktic foraminiferal tests (foraminiferal packstone). This sediment is cross-bedded and burrowed (Fig. 3). Burrows are approximately 5 mm in diameter, unbranched, and reach a length of a few centimeters. Most are horizontal or oblique, but a few almost vertical shafts initiate in the upper surface of the bioclastic layer. Even these tubes are packed with yellow foraminiferal sand and none with the green clay that overlies the calcarenitic layer. The upper surface of the yellow calcarenitic marly limestone is undulating and likely represents an erosional disconformity.

A plastic green clay, between 0.2 and 1 cm thick, fills the depressions of the calcarenite and underlies a 2–4 mm thin rust-colored ferruginous layer interpreted as the K–T boundary red layer.

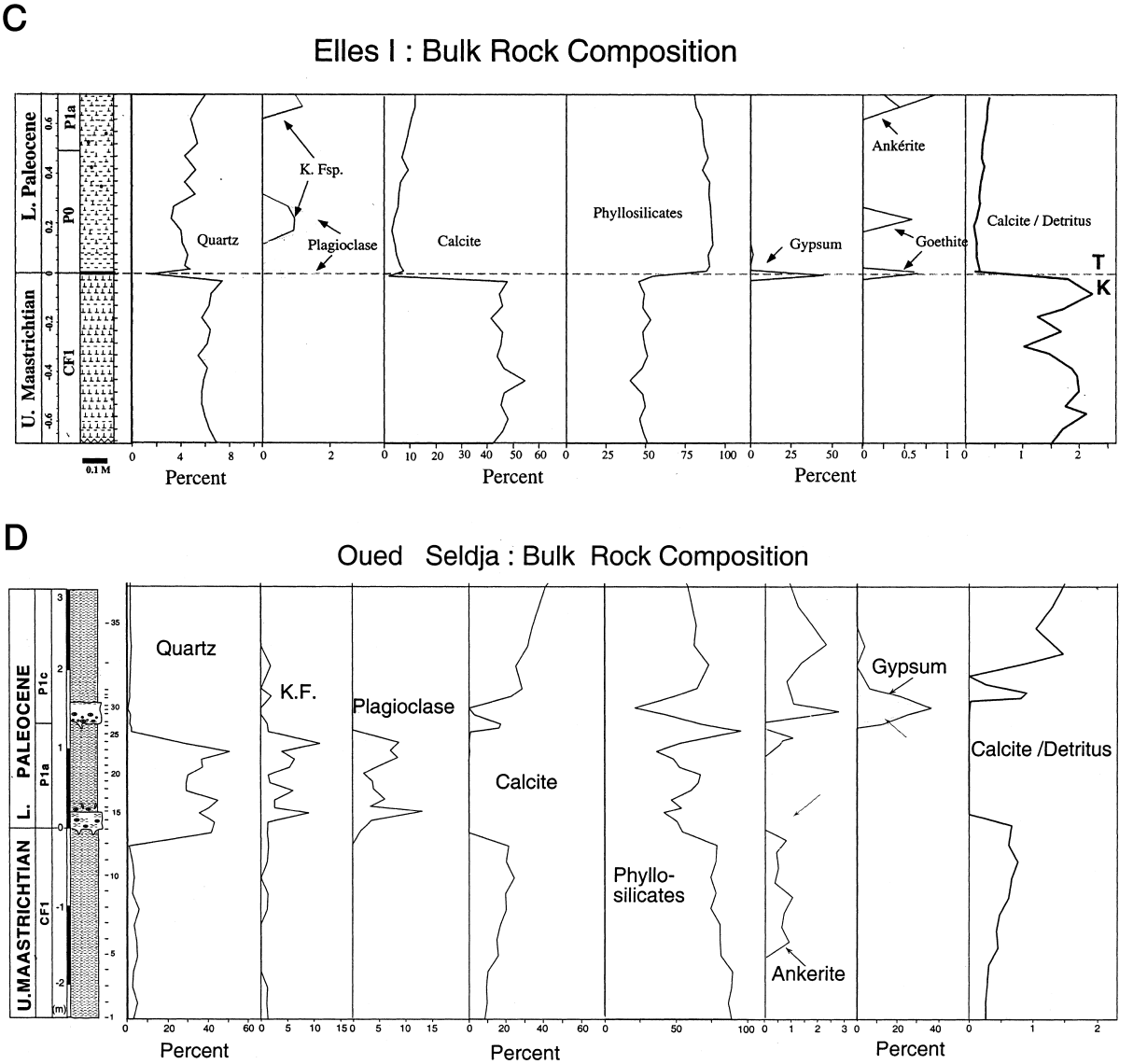

No burrows appear to be present in the green clay and none cross through the red layer. Overlying the red layer is a 1–2 cm thick plastic green clay followed by a second very thin layer of rust-colored ferruginous material and a gypsum goethite crust (Fig. 3). Upsection, the clay grades into dark fissile shales with small goethite concretions (Zone P0). The lowermost 10 cm of these shales are black, rich in organic matter, and contain rare casts of nuculanid bivalves. The fissile black shales grade into gray and light gray shales which are less fissile for several meters upsection. Bioturbation first reappears at 50 cm above the red layer. The stratigraphic interval considered in this paper covers the uppermost meter of the Maastrichtian (CF1), the K–T boundary (P0) and the first meter of the Danian (P1a) (zonation after Keller et al., 2002).

Paleoceanographically, the Elles section was located closer to the emerged areas of the Kasserine Island and hence received a higher influx of detritus than El Kef (Burollet, 1956). Paleodeposition

occurred in a middle to outer neritic environment (100–250 m). Due to the proximity to the Kasserine Island, sediment accumulation rates are significantly higher than at El Kef with an average of 3 cm/ka at Elles II for Zone CF1, as compared with 2cm/ka for El Kef for the equivalent interval, and 2.3 cm/ka for the P0–P1a interval as compared with 1.9 cm/ka for El Kef (time scale based on Cande and Kent, 1995).

3.4. Ain Settara K–T

The Ain Settara section is located in the Kalaat-Senan area about 50 km southeast of El Kef and northwest of Elles (Fig. 1, see Dupuis et al., in press, for precise location). Only the top 60 cm of the upper Maastrichtian gray silty marls were collected. At the top of this interval, and about 2 cm below the K–T red layer and dark clay is a weak disconformity marked by truncated *Chondrites* burrows (unbranched). A 2 cm thick dark silty shale overlies the disconformity (Figs. 2, 3). The top of this silty shale is also marked by *Chondrites* burrows some of which are vertical, truncated and infilled with the overlying dark clay. This suggests another disconformity centered at the K–T boundary.

Similar to Elles I, the K–T transition is characterized by a 0.3–0.5 cm thick red layer sandwiched between two thin layers of secondary gypsum, goethite and jarosite. No burrowing is observed across the red layer and in the overlying dark 2 cm thick boundary clay. Above the boundary clay layer is a 1.5 cm thick silty layer containing coarser grains of mainly diagenetic calcite (Fig. 3). This silt layer has been interpreted as a small storm deposit by Dupuis et al. (in press). The presence of reworked transported species in the sample from this layer confirms the resedimented nature of this event bed which represents higher hydrodynamic conditions at the P0/P1a boundary (Luciana, 2002). It is likely that this event also represents an erosional disconformity which could be responsible, at least in part, for the unusually thin boundary clay (2 cm thick) in this section, as compared with Elles and El Kef. Upwards, the 70 cm sediments analyzed grade from dark gray fissile shaley clay to gray (sometimes silty) shale.

The Ain Settara section was deposited in a more proximal environment to the Kasserine Island than either Elles or El Kef and at inner to middle neritic paleodepths. The largely missing Zone P0 interval and very low sedimentation rate in Zone P1a (0.9 cm/ka) reflect hiatuses at the K–T boundary and at the top of Zone P0.

3.5. Seldja K–T

Oued Seldja is located about 200 km from El Kef, in a gorge near Metlaoui (for directions see Keller et al., 1998). The outcrop spans the south flank of a W–E stiking anticline and the beds dip steeply (60–80°) to the south. The uppermost Maastrichtian interval consists of 2.4 m of gray to brown silty shales, clays and clayey siltstones which are overlain by a 15 cm thick bed of yellow silty sandstone rich in reworked fish scales and teeth. The undulating contact between these lithologies indicates erosion as also suggested by truncated burrows and the presence of mud clasts from the underlying sediments within the sandstone layer (Figs. 2, 3, Keller et al., 1998). Above this layer are 1.15 m of gray silty shales and clays that contain early Danian (Zone Pla) planktic foraminiferal assemblages. This interval is followed by a 25 cm thick bed of gray sandy phosphate. The lower contact of this bed is marked by an undulose surface, manganese crusts and nodules that suggest an extended period of erosion and non-deposition. The lower 5 cm of the phosphate layer contain mud clasts and phosphate-filled burrows extended into the underlying shales. The phosphate layer is rich in fish remains (shark teeth, fish scales), small bivalves (mostly nuculanids) and gastropods. The first 5 cm above the phosphate layer consist of gray-green marly siltstone rich in microfossils (foraminifera and ostracods) with small (0.5–1 cm) clasts of phosphate. Upsection, marly siltstones (P1c) grade into brown siltstone with increasingly abundant terrestrial plant debris.

During the K–T transition, the sediments were deposited in the shallow Gafsa Basin at inner neritic depths (Fig. 1). To the south, the basin was connected to the evaporite Sahara platform which was separated from the Tethyan realm to the

north by the Kasserine Island. The interchange with the open sea was therefore restricted and probably further hampered by small uplifted areas to the east and west which could have acted as barriers to circulation (Burollet, 1956; Burollet and Oudin, 1980; Sassi, 1974). Sediment deposition occurred largely in restricted seas that fluctuated between inner neritic to coastal environments. Tectonic activity and erosion of the Kasserine Island contributed to a constant though variable terrigenous influx of sediments. No sediment accumulation rate has been calculated due to the numerous hiatuses detected in this section.

4. Bulk rock mineralogy

The dominant bulk rock composition of the K–T transitions in Tunisia is calcite and phyllosilicates, with minor amounts of quartz, feldspar (plagioclase and K-feldspar) and phosphate (F-Ca apatite). Ankerite (Fe-rich dolomite) and pyrite are sometimes present. Gypsum and hydroxide minerals such as goethite and jarosite are generally restricted to the K–T boundary clay. These minerals are of secondary origin and reflect late diagenetic processes.

At El Melah, the K–T transition is marked by a sharp change in the bulk rock composition (Fig. 4A). Zone CF1 below the K–T boundary contains significant calcite (40–50%) and phyllosilicates (50–60%) with minor quartz (5–7%) and plagioclase (1%). At the K–T boundary, calcite and quartz drop abruptly to 1%, whereas phyllosilicates and gypsum increase to 80 and 2%, respectively. In the upper part of Zone P0, calcite increases to 20% and quartz to 6–7%, but both decrease at the P0–P1a transition. A short-term increase in calcite (46%) in the first 10 cm of Zone P1a parallels a decrease in phyllosilicates. Upsection between Pla and the lower part of Plc, phyllosilicates decrease and calcite gradually increases with a temporary peak in Zone P1b (55–60%). Higher quartz (8–10%) and plagioclase (1–2%), but lower calcite (20–30%), mark the upper part of Plc, except for peak abundance (85%) near the top of the section which marks the onset of alternating deposition of marl and marly limestone layers that spans through the P1d–P2 interval.

At El Kef and Elles, bulk rock compositions differ from El Melah primarily in the continued low calcite values through Zones P0 and Pla (Fig. 4B, C). This difference, however, may be largely due to the more condensed section at El Melah where P0 is only 10 cm thick and Pla is less than 1.5 m thick. The overall bulk composition during the uppermost Maastrichtian Zone CF1 at El Kef is similar to El Melah, with relatively high calcite (40–57%) and phyllosilicates (42–57%) and minor quartz (2–4%, Fig. 4B). Though in the top 30 cm of Zone CF1, calcite increases significantly (from 40 up to 57%) and then decreases (46%) 5 cm below the K–T boundary clay layer. This calcite peak coincides with higher quartz (4%) and lower phyllosilicates (35–40%) and corresponds to a similar interval at Elles II. At the K–T boundary, calcite drops to 5% at El Kef with phyllosilicates (37%) and gypsum (37%) abundant. Goethite is present just below and above the clay layer (1–2%). In the expanded Zone P0 at El Kef (and Elles), calcite remains low (2–3%) and phyllosilicates reach maximum values (96%). The first significant increase in calcite (up to 10%) coincides with decreased phyllosilicates at 47 cm above the clay layer. At the P0–P1a transition, calcite decreases (3%) and phyllosilicates and quartz increase. Phyllosilicates (87–90%) reach maximum abundance in the lower part of Zone P1a, followed by calcite (3–9%) and quartz (3–4%). Calcite increases significantly (30–40%) 3 m above the K–T clay layer up to the middle part of P1b, whereas quartz and phyllosilicates are less abundant with 2 and 50–60% respectively. Small amounts of ankerite ($>2\%$) coincide with these calcite maxima. The upper part of P1b and the base of P1c Zones are again marked by decreasing calcite (18–25%) and coeval increasing detrital input (Fig. 4B).

At Elles I and II the K–T transition is marked by a sharp change in bulk rock composition, similar to El Kef and El Melah (Fig. 4C). The uppermost Maastrichtian Zone CF1 is characterized by relatively high calcite and phyllosilicate contents (40–60%) and minor quartz (4–7%); feldspars, goethite, jarosite and gypsum are not present in

that part of the section. There is an increase in calcite (from 39 to 45%) 8 cm below the K–T, coinciding with a decrease in phyllosilicates. The K–T boundary clay layer contains very little calcite (1–2%) and quartz (2%), but abundant phyllosilicates (52%) and gypsum (45%). Plagioclase (2%) and hydroxide minerals, such as goethite (1%) and gypsum of secondary origin are present and reflect late diagenetic processes. At Elles, similar to El Kef, calcite remains low ($<15\%$) through Zone P0 and the lower part of P1a and detrital influx is minor (quartz $<4\%$, K-feldspar 2%, plagioclase $<3\%$, Fig. 4B, C).

At the shallow inner neritic Seldja section, calcite deposition is nearly half (20–25%) of that in deeper water sections to the north (Fig. 1), whereas phyllosilicate deposition is higher ($>70\%$, Fig. 4D). Above the disconformity which marks the K–T boundary (Pla/CF1), there is a major change in bulk rock composition to dominant quartz (30–50%) and phosphate, increased feldspar and plagioclase (11 and 13% respectively) and decreased phyllosilicates ($<50\%$). The overlying 25 cm thick silty phosphate layer (Zone Pla) contains 16% calcite, 60% phyllosilicates, low quartz and feldspar, and the first occurrence of phosphate (F-Ca apatite). A 30 cm thick phosphate layer ($\sim$37% phosphate) marks a disconformity between Zones Pla–Plc. Near the top of the phosphate layer gypsum of late diagenetic origin is abundant (28–38%), whereas phyllosilicates (60%) and calcite (40%) dominate above this interval.

Bulk rock and clay mineral compositions have not been measured by us for the Ain Settara section. These data have been processed by Dupuis et al. (in press).

5. K–T sea-level changes: bulk rock mineralogy

Sea-level changes are commonly recognized from field-based observations of lithological characteristics and laboratory analysis of bulk rock compositions. In open marine settings, the carbonate/detritus (mainly phyllosilicates and quartz) ratio is a useful index for sea-level fluctuations. Increased carbonate content reflects generally a more distant detrital source and thus deeper water conditions, whereas an increase in detritus indicates a more proximal source and consequently a lower sea-level or shallower water environment. Hiatuses or disconformities are indicated by non-deposition and erosion surfaces, including burrowed or semi-lithified omission surfaces in deeper waters. Bored and encrusted hardgrounds with phosphate and/or glauconite indicate shallow water environments, non-deposition and less commonly flooding surfaces (Donovan et al., 1988; Loutit et al., 1988; Robaszynski et al., 1998; Vincent et al., 1998). Calcisiltite and calcarenitic marly limestones enriched in foraminifera, such as those observed near the top of the Maastrichtian at El Kef and Elles, represent current winnowing which is commonly associated with transgressive system tracts. In addition to these major sedimentary criteria, variations in the kaolinite/smectite (K/SM) ratio can also be used to infer the proximity of the source area. Since kaolinite is more abundant in coastal areas and smectite in open marine environments, the K/SM ratio may also reflect sea-level changes, in addition to climatic variations (Adatte and Rumley, 1989; Chamley et al., 1990).

Recognition of sea-level fluctuations in our sections is thus based on lithological characteristics (e.g. hardgrounds, erosional surfaces, particle size variations) and the ratio of calcite/detritus (where

Fig. 5. Sea-level changes across the K–T transition at El Melah, El Kef, Elles and Seldja based on lithological variations, biostratigraphic data and bulk rock compositions (calcite/detritus ratios). In open marine settings, the calcite/detritus ratio (mainly phyllosilicates and quartz) is a useful index for sea-level fluctuations. Increased carbonate content reflects a more distant detrital source and thus deeper water conditions, whereas an increase in detritus indicates a more proximal source and consequently a lower sea-level or shallower water environment. Note that the K–T boundary corresponds to a transgressive interval. The calcite/detritus ratio indicates sea-level lowstands in Zones CF1, near the P0–Pla and P1b–P1c transitions. Note that two hiatuses are present at Seldja, at the K–T boundary (Zones P0, the lower part of Pla and upper part of CF1 are missing) and in the Danian where Zone Plb and upper part of Pla are missing.

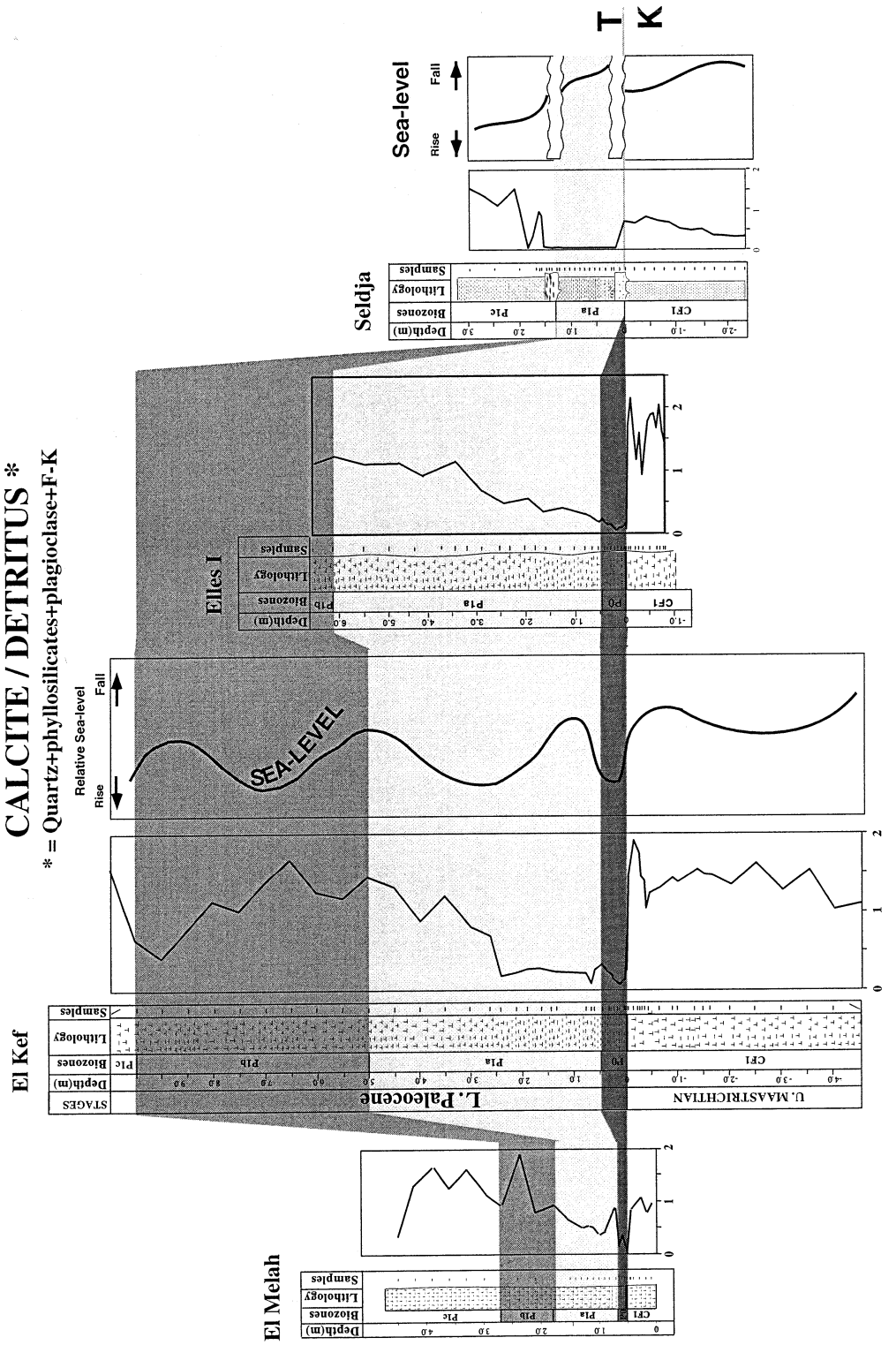
CALCITE / DETRITUS *
* = Quartz+phyllosilicates+plagioclase+F-K
Relative Sea-level
Rise
Fall
SEA-LEVEL
El Kef
El Melah
Elles I
Seldja
Sea-level
T
K
U. MAASTRICHTIAN
L. Paleocene
STAGES
Depth(m)
Biozones
Lithology
Samples
CF1
P0
Pla
Plb
Plc

detritus includes quartz, phyllosilicates, plagioclase and K-feldspar). Increased abundance of detritus may reflect increased erosion and lower sea-levels, whereas increased calcite and decreased detritus suggest decreased erosion during higher sea-levels. In addition, sea-level changes differentially influence sediment deposition at various paleodepths with sediment starvation occurring during sea-level rises and sediment erosion during falls, particularly in shallow neritic areas. The Tunisian sections analyzed span sedimentary environments from inner neritic to middle and outer neritic and upper slope settings (Fig. 1) and provide strong evidence for sea-level fluctuations across the K–T boundary.

The calcite/detritus ratio in the Tunisian sections (Fig. 5) correlates with sea-level changes inferred from lithological and biostratigraphic data. At El Kef and Elles, this ratio averages 1.5 and 2 respectively during the upper Maastrichtian (upper CF1) and indicates a relatively high sea-level with significant terrigenous influx from the nearby Kasserine Island (Fig. 1). In both sections the calcite/detritus ratio decreases to 1.0 between 50–100 cm below the K–T boundary and suggests a lower sea-level accompanied by increased detrital influx (Fig. 5). Within the top 30–40 cm of the Maastrichtian the calcite/detritus ratio increased to about 2.0 and reflects a significant sea-level rise which correlates with the foraminiferal packstone at El Kef and Elles (Fig. 3). Increased smectite in this interval (Fig. 6) suggests that this sea-level rise was accompanied by drier climatic conditions (Chamley, 1989). The foraminiferal packstone likely accumulated by current winnowing and suggests the onset of a period of starvation in the basin. At Elles I and II the packstone is marked by an undulating lower surface that suggests erosion. An erosion surface is also present just below the K–T boundary at Ain Settara (Fig. 3). At El Melah, the foraminiferal packstone is not observed and its absence is likely due to the deeper water setting at this location. At Seldja, this interval may be missing due to a hiatus that spans the K–T boundary, though increasing calcite/detritus values near the top of the Maastrichtian also suggest a rising sea-level (Fig. 5).

The sea-level rise that began just below the K–T boundary reached a maximum in Zone P0 as suggested by condensed clay deposition worldwide (Brinkhuis and Zachariasse, 1988; Keller, 1988a,b; Donovan et al., 1988; Baum and Vail, 1988; Keller and Stinnesbeck, 1996; Stinnesbeck et al., 1996). The very low carbonate content in Zone P0 is likely related to the mass extinction of tropical and subtropical planktic foraminifera and calcareous nannofossils (Keller et al., 1995; Luciana, 2002; Pospichal, 1994). The upper part of P0 is missing in the shallower sections of Ain Settara where P0 is only 3 cm thick, and at Seldja where P0 is missing (Fig. 3). These hiatuses mark a sea-level lowstand and erosion in shallow water sections at the P0–Pla boundary. A short hiatus at the P0–Pla boundary has been observed in sections worldwide (MacLeod and Keller, 1991a,b; Schmitz et al., 1992; Keller et al., 1993; Keller, 1993).

A rising sea-level is indicated in Zone Pla marked by increasing calcite deposition and increasing calcite/detritus ratios which reach a maximum in Zone Plb (Fig. 5). A sea-level lowstand and short hiatus is associated with the Pla–Plb boundary in many sections (Macleod and Keller, 1991a,b; Keller and Benjamini, 1991; Canudo et al., 1991; Keller and Stinnesbeck, 1996), though not observed in Tunisia, except at the shallow neritic Seldja section. At Seldja, Plb and much of Pla is missing due to a hiatus (Fig. 5). At the Plb–Plc boundary the calcite/detritus ratio decreases to < 0.5 at El Kef and El Melah indicating increased terrigenous influx and a lower sea-level. A hiatus is widespread at the Plb–Plc boundary (MacLeod and Keller, 1991b), including at Seldja and reflects a major sea-level regression.

6. K–T climate changes: clay mineralogy

Clay mineral assemblages reflect continental morphology and tectonic activity, as well as climate evolution and associated sea-level fluctuations (Chamley, 1989, 1997; Weaver, 1989; Li et al., 2000). Illite and chlorite are considered common byproducts of weathering reactions with low hydrolysis typical of cool to temperate and/or dry

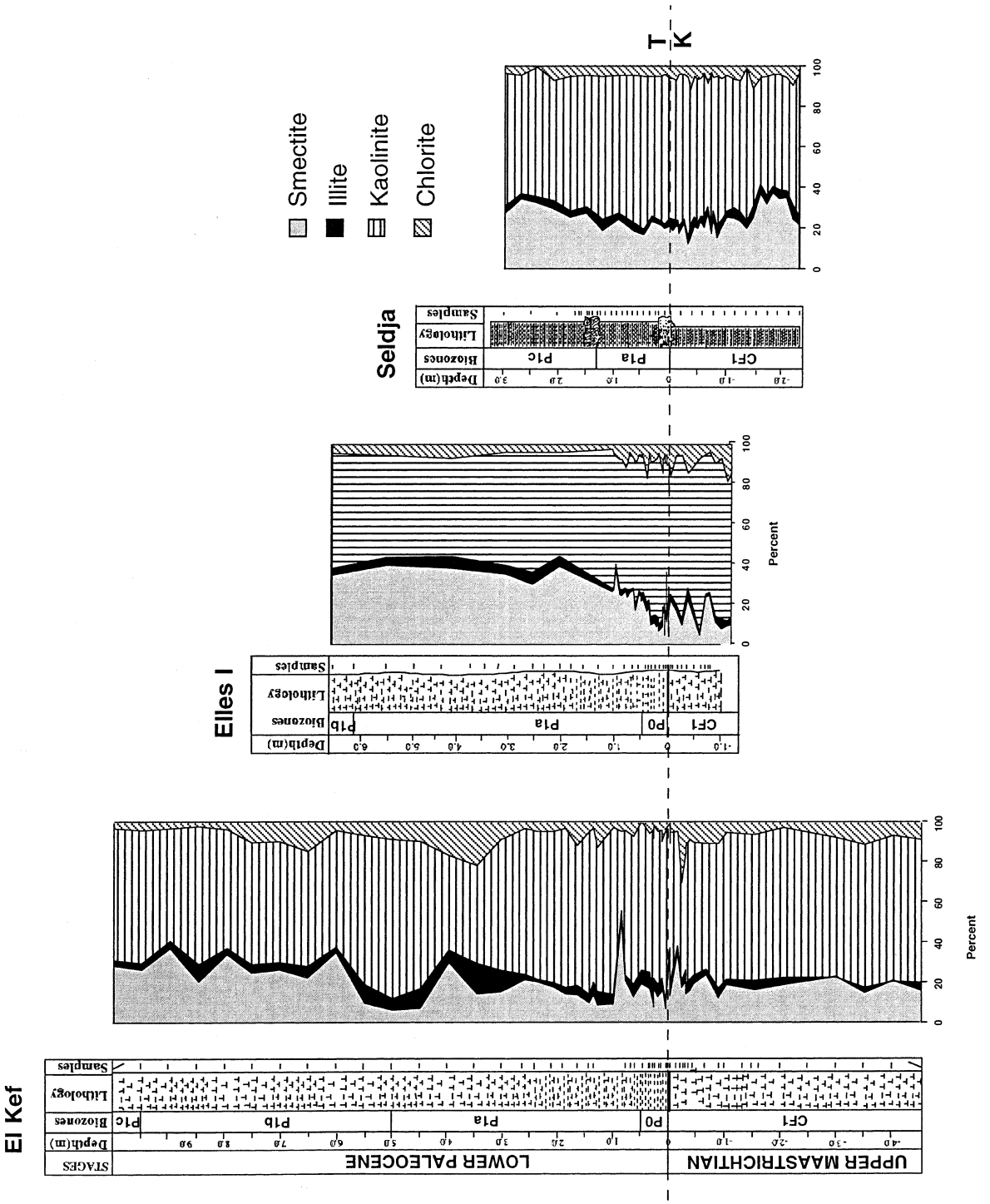

Fig. 6. Clay mineral compositions (>2 μm clay fraction, relative abundance) across the K–T transition at El Kef, Elles and Seldja. Note the peaks in smectite just below and at the K–T boundary and in the lower part of Zone P1a at El Kef and Elles. Smectite content is lowest just above the K–T boundary and Zone P0 and gradually increases in Zone Pla.

climates. Kaolinite is generally a byproduct of highly hydrolytic weathering reactions in perennially warm humid climates and its formation requires a minimum of 15°C (Gaucher, 1981). The presence of abundant smectite is generally linked to transgressive seas and warm climate with alternating humid and arid seasons, but can also reflects volcanic activity (Chamley, 1989, 1997; Deconinck, 1992). The kaolinite/smectite ratio is a climate proxy that reflects humid/warm to more dry and seasonal climate variations (e.g. Robert and Chamley, 1991; Robert and Kennett, 1992). The ratio of kaolinite to smectite (K/SM) can therefore be used as proxy for climate change.

6.1. Clay mineral results

Kaolinite is the most abundant clay mineral (mean value of 67%) in the K–T transitions of Tunisia. Smectite, chlorite and mica are minor components and average 18, 11 and 4%, respectively. All identified clay minerals are known from normal deposition or pedogenic environments and exist in various amounts within Cretaceous and Paleogene sediments. Smectite is absent at El Melah probably due to post-depositional burial linked with increased tectonic activity (Tell thrusting, Burollet, 1956). Relative abundances and clay mineral ratios of the El Melah section are therefore not comparable with other sections and hence not included in the following discussion.

At El Kef, Elles and Seldja the uppermost Maastrichtian (CF1 Zone) sediments are dominated by kaolinite ($>65\%$) and variable (10–38%) but gradually increasing smectite contents (Fig. 6). Chlorite is variable ($<20\%$), but reaches maximum values (30%) just below the K–T boundary at El Kef and decreases upsection. The variability in smectite and chlorite is generally compensated by decreasing or increasing kaolinite in all sections. Mica is generally a minor component. Similar smectite and kaolinite averages persist in the K–T boundary clay layer, though smectite is generally high ($\sim$38% at Elles). In Zone P0 smectite significantly decreases (to $\sim$10–15%) at El Kef and Elles (P0 is missing at Seldja) and kaolinite increases (up to 85%), whereas chlorite remains low (3–7%). About 40 and 30 cm above the P0–P1a transition smectite briefly peaks at 51% at El Kef and at 40% at Elles respectively (Fig. 6). Thereafter, smectite decreases to 9% at El Kef and then gradually increases to 40% with peak abundance in chlorite and minimum values (47%) in kaolinite. At Elles, smectite gradually increases in the lower part of Pla and reaches maximum values of 38% similar to El Kef. At Seldja, most of Zone Pla is missing and the interval present averages 20% smectite and 70% kaolinite. At El Kef, the P1a–P1b transition is characterized by decreased smectite (7%) and increased kaolinite (80%). Smectite increases upsection to an average of 29% in Zone P1b and kaolinite decreases to an average of 55%. Similar values are observed in Zone Plc at Seldja (Fig. 6).

6.2. Inferred climate changes

During the latest Maastrichtian to early Danian, the Tunisian sections were located on a continental platform which experienced little hydrodynamic activity and hence little mineral segregation that could mask or exaggerate the climate signal (Adatte and Rumley, 1989; Chamley, 1989; Monaco et al., 1982). Since kaolinite is usually more abundant in coastal areas and smectite in open marine environments, the K/SM ratios may also reflect sea-level changes. But primarily, variations in K/SM ratios are linked to climate changes. The smectite from the K–T layer is identical to the smectite within uppermost Maastrich-

Fig. 7. Kaolinite/smectite ratios across the K–T transition at El Kef, Elles and Seldja and inferred climatic evolution. The high K/SM ratios, the low content in chlorite with mica nearly absent indicate an overall warm and humid climate from the upper Maastrichtian Zone CF1 to the lower Paleocene Zone P1c. Note the four maxima in kaolinite/smectite ratio observed in the topmost Maastrichtian, in the upper part of P0, in the lower part of P1a and at the P1a/P1b transition (El Kef), reflecting more humid conditions. A sea-level curve based on various sedimentological, biostratigraphical and geochemical proxies is superimposed over the K/SM ratio for El Kef. Decreases in K/SM ratios correspond to generally increased smectite during transgressive intervals under more seasonal conditions.

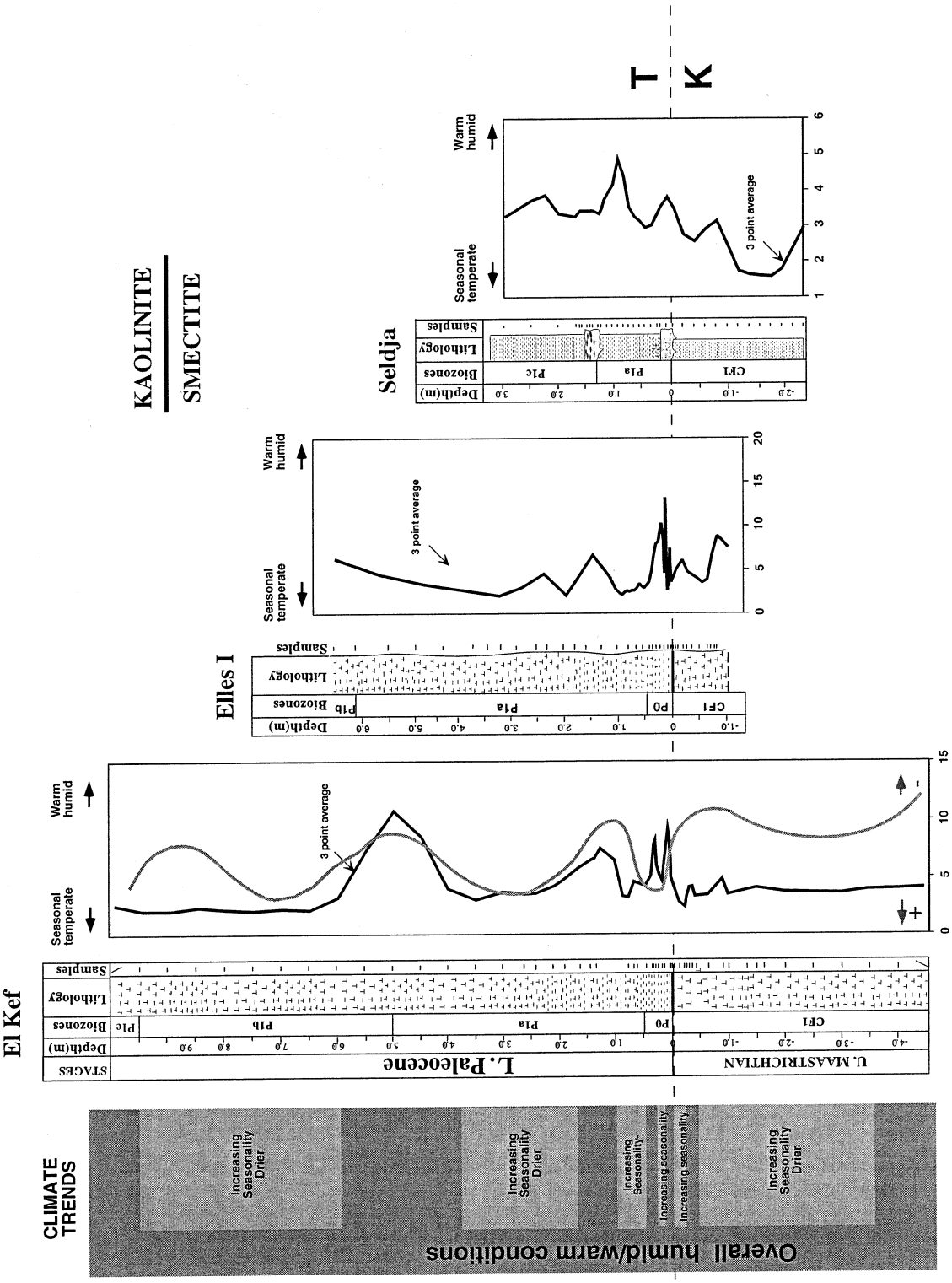
CLIMATE TRENDS
Overall humid/warm conditions
Increasing Seasonality Drier
Increasing Seasonality
Increasing seasonality
Increasing seasonality
Increasing Seasonality Drier
El Kef
STAGES
U. MAASTRICHTIAN
L. Paleocene
Depth(m)
Biozones
CF1
P0
P1a
P1b
P1c
Lithology
Samples
Seasonal temperate
Warm humid
3 point average
Elles I
Seldja
KAOLINITE
SMECTITE
T
K

tian and earliest Danian sediments. ESEM and EDX analyses reveal a Fe-Al enriched and not well crystallized smectite which typically develops in soils under intermediate climatic conditions with seasonal contrasts (Chamley, 1989, 1997). At Elles and El Kef, the high K/SM ratios, the low content in chlorite with mica nearly absent indicate an overall climate trend characterized by humid and warm conditions across the K–T transition (Zones CF1 to P1c, Figs. 7 and 11). Within this interval are four K/SM maxima located respectively 80 cm below the KTB, in the lower part of P0, in the lower part of P1a and at the P1a–P1b transition (Figs. 7, 8A). The second K/SM maximum, located in the lower part of P0 just above the red clay layer, has also been observed at Caravaca (Kaiho et al., 1999). Within this main trend, relatively low K/SM ratios are located at 15–20 cm below the K–T red layer, near the P0–P1a transition, in the middle of P1a and in P1b. These K/SM minima indicate, within the overall humid condition trend, periods of increasing seasonality and possibly drier climatic conditions. These relatively low K/SM ratios correlate with high sea-levels observed in sections globally (MacLeod and Keller, 1991a,b; Keller and Stinnesbeck, 1996) and also inferred based on the calcite/detritus ratio in this study.

At El Kef and Elles, relatively low K/SM ratios in the uppermost part of CF1 suggest increased seasonal alternations in the rainfall regime (ST, Fig. 7). The subsequent sea-level transgression marked by the foraminiferal packstone (top 40 cm of Zone CF1 at El Kef and top 25 cm at Elles), is associated with increased kaolinite followed by a decrease 15–20 cm below the KT red layer (Fig. 6). The kaolinite decrease (to 50%) coincides with a strong increase in smectite (to 40%) which persists into the K–T clay layer at El Kef and Elles. At both El Kef and Elles sections, the K/SM ratios in Zone P0 (Fig. 7) suggest a series of alternating warm humid (WH) and seasonally wet (ST) climate fluctuations beginning at the K–T boundary with the first 2–10 cm warm and humid, between 10–20 cm seasonally temperate, 20–35 cm warm humid, 35–70 cm seasonally temperate (Fig. 7). These clay mineral variations reflect alternating drier and more humid conditions on land during the first 30–40 ka of the Danian. Peak K/SM ratios are also observed in the lower part of Zone Pla, about 1.5 m above the K–T boundary at Elles and El Kef, and suggest an interval of warmer humid climate (Fig. 8a). At Seldja, the peak K/SM ratio in Zone Pla at 80 cm above the K–T boundary may correlate this warm humid period (upper part of Pla is missing at Seldja). Lower K/SM ratios during most of Zone Pla at Elles and El Kef suggest a drier climate with increasing seasonality. At El Kef, a maxima in the K/SM ratio at the Pla–Plb boundary marks increased precipitation and is associated with a lower sea-level and high detrital influx. At Seldja, a maximum in kaolinite is observed in the phosphatic sandstone of Zone P1c (Fig. 6) which reflects a condensed interval during a rising sea-level. These data suggest that the climate across the K–T transition (Zones CF1 to Plc) in Tunisia alternated between warm and humid periods and drier periods with increasing seasonality. In general, warm/humid (perennially wet) periods coincide with low sea-levels, whereas increased seasonality and drier climates coincide with higher sea-levels inferred from bulk rock compositions (Fig. 8B).

7. Organic matter

Total organic carbon (TOC) in marine sediments is generally a geochemical proxy for primary productivity and carbon burial linked to climate, erosion and sea-level fluctuations. During low sea-levels, or perennially wet climates, TOC values are generally high as a result of enhanced terrestrial organic matter influx associated with increased erosion and carbon burial. During high sea-levels, TOC values are generally lower, except in special circumstances, such as the K–T boundary clay where organic carbon is concentrated at a flooding surface associated with decreased productivity or anoxia.

Average values of total organic carbon (TOC) are relatively high at El Kef and Elles (0.45–0.50%), but relatively lower at El Melah (0.30%) and Seldja (0.20%, Fig. 9). In the uppermost 20–30 cm of the Maastrichtian (CF1), TOC values

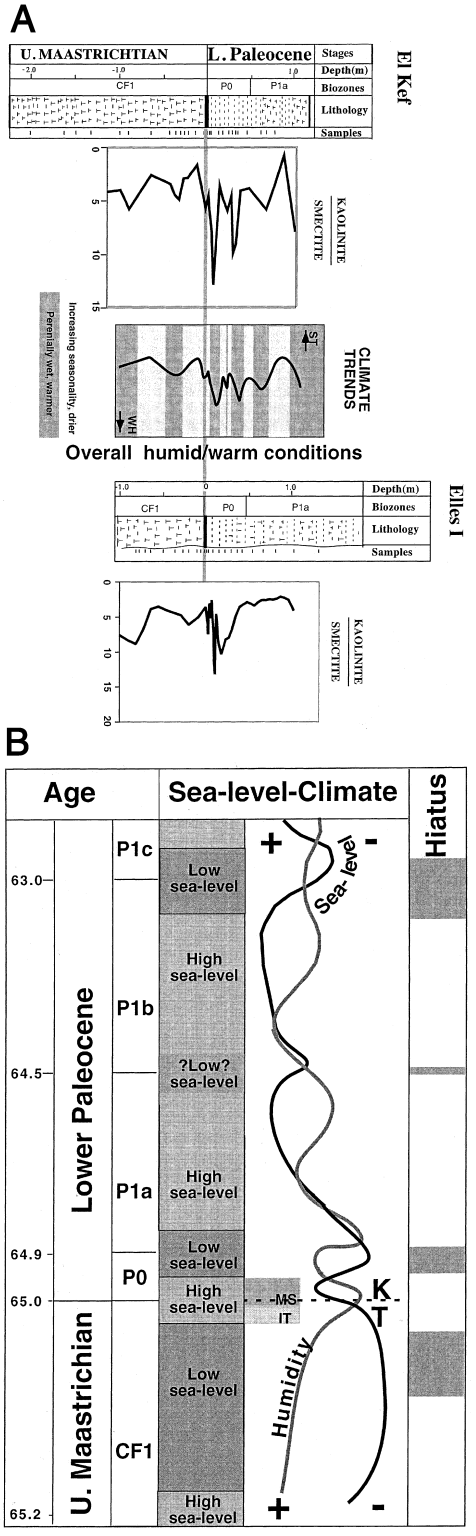

Fig. 8. (A) Short-term trends in the kaolinite/smectite (K/SM) ratio at El Kef an Elles, suggesting a series of alternating perennially wet (WH) and seasonal temperate (ST) climate at the KT transition. (B) Summary of hiatuses based on biostratigraphic data and sedimentological observations (e.g. disconformities, truncated burrows, lithological changes), sea-level changes inferred from bulk rock compositions, lithological and sedimentological characteristics and biostratigraphy, and climate changes inferred from clay mineral data across the K–T transition in Tunisia. Note that short hiatuses are identified at the top of Zone CF1 (Seldja, Ain Settara, Elles), at the P0/P1a, Pla–Plb and P1b–P1c boundaries, all of which correlate with low sea-levels and have been recognized globally (MacLeod and Keller, 1991a,b; Keller and Stinnesbeck, 1996). The P1a–P1b hiatus is not well developed in Tunisia. High sea-levels generally correspond to increasing seasonality and drier conditions, whereas low sea-levels correspond to increasing humidity and possibly warmer conditions.

increase and reach maximum values in the K–T boundary red clay layer in all sections, except Seldja where this interval is missing. The red clay layer is therefore marked in all sections by maximum TOC values (1.5% at El Kef, 0.65% at El Melah, 0.8% at Elles). At Elles and El Kef, TOC values decrease in Zone P0 to an average of 0.45% and at El Melah to 0.20%. Upsection in Zones Pla–Plb, TOC contents fluctuate between 0.15 and 0.7% at El Kef and 0.1 and 0.35% at El Melah.

At Elles and El Kef, the relatively high average TOC values recorded in the P0 Zone can be explained by sediment starvation during sea-level rise. At Seldja, organic matter is lower due to erosion and oxidation. At El Kef and Elles, the overall TOC trend indicates the continuous presence of significant organic matter with a maximum coinciding with the K–T boundary. These relatively high TOC values agree well with the perennially wet and warm climate inferred from clay minerals and the associated accelerated runoff from continents which prevailed during the uppermost Maastrichtian. TOC contents increase at El Melah, El Kef and Elles about 30–40 cm below the K–T boundary, coincident with the onset of the transgressive interval which culminates in the K–T clay layer (P0). Maximum TOC content in P0 may be of multiple origins, including

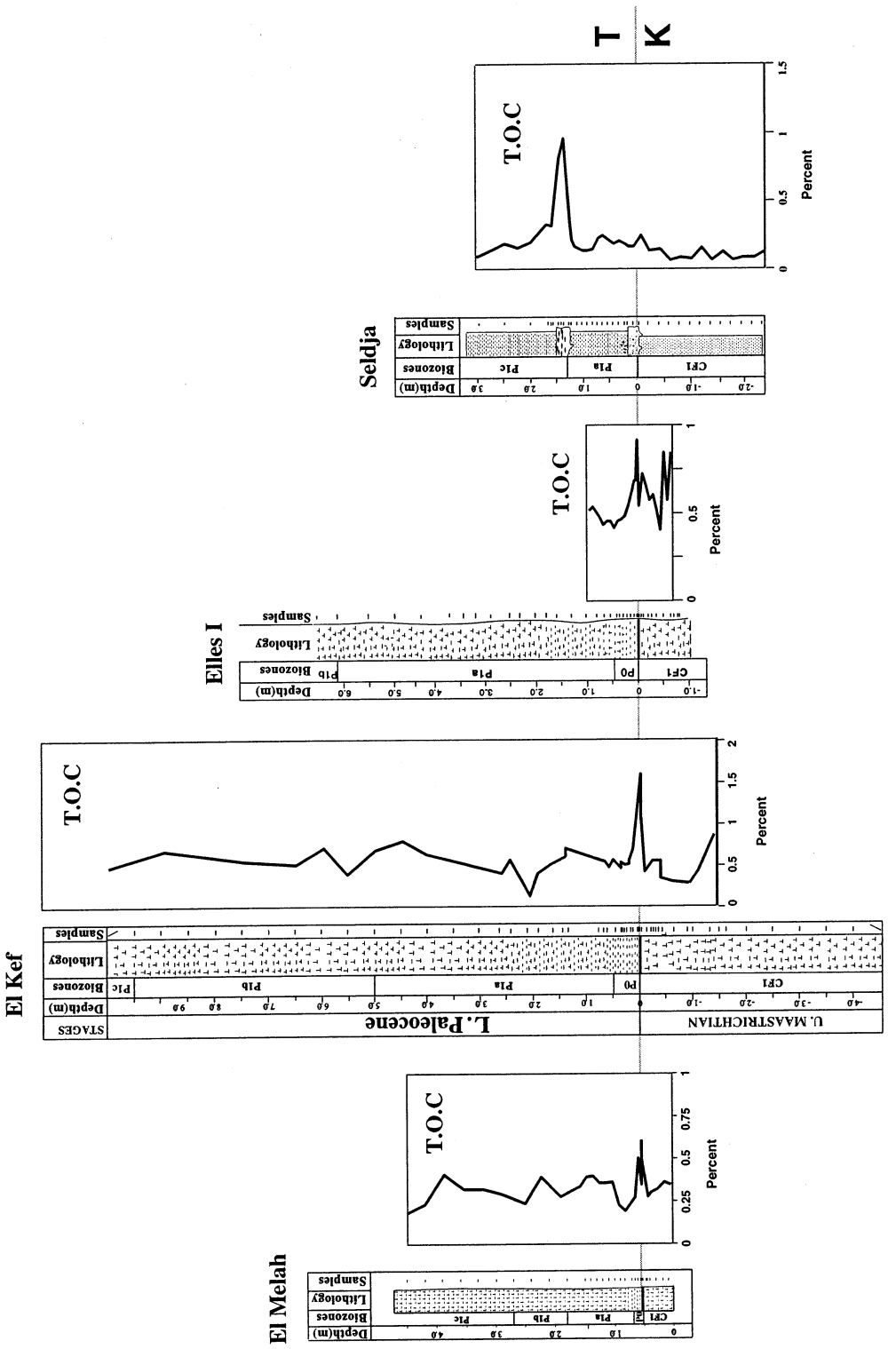
T
K
T.O.C
Percent
Seldja
Depth(m)
Biozones
Lithology
Samples
CF1
P1a
P1c
T.O.C
Percent
Elles I
Depth(m)
Biozones
Lithology
Samples
CF1
P0
P1a
P1b
T.O.C
Percent
El Kef
STAGES
Depth(m)
Biozones
Lithology
Samples
U. MAASTRICHTIAN
L. Paleocene
CF1
P0
P1a
P1b
P1c
T.O.C
Percent
El Melah
Depth(m)
Biozones
Lithology
Samples
CF1
P1a
P1b
P1c

Fig. 9. Total organic carbon content (TOC) across the K–T transition at El Melah, El Kef, Elles and Seldja. Note that TOC content begins to increase just before the K–T boundary and reaches maximum values at the K–T boundary layer. Peak TOC values at the Pla–Plc hiatus interval at Seldja mark a phosphate-rich layer.

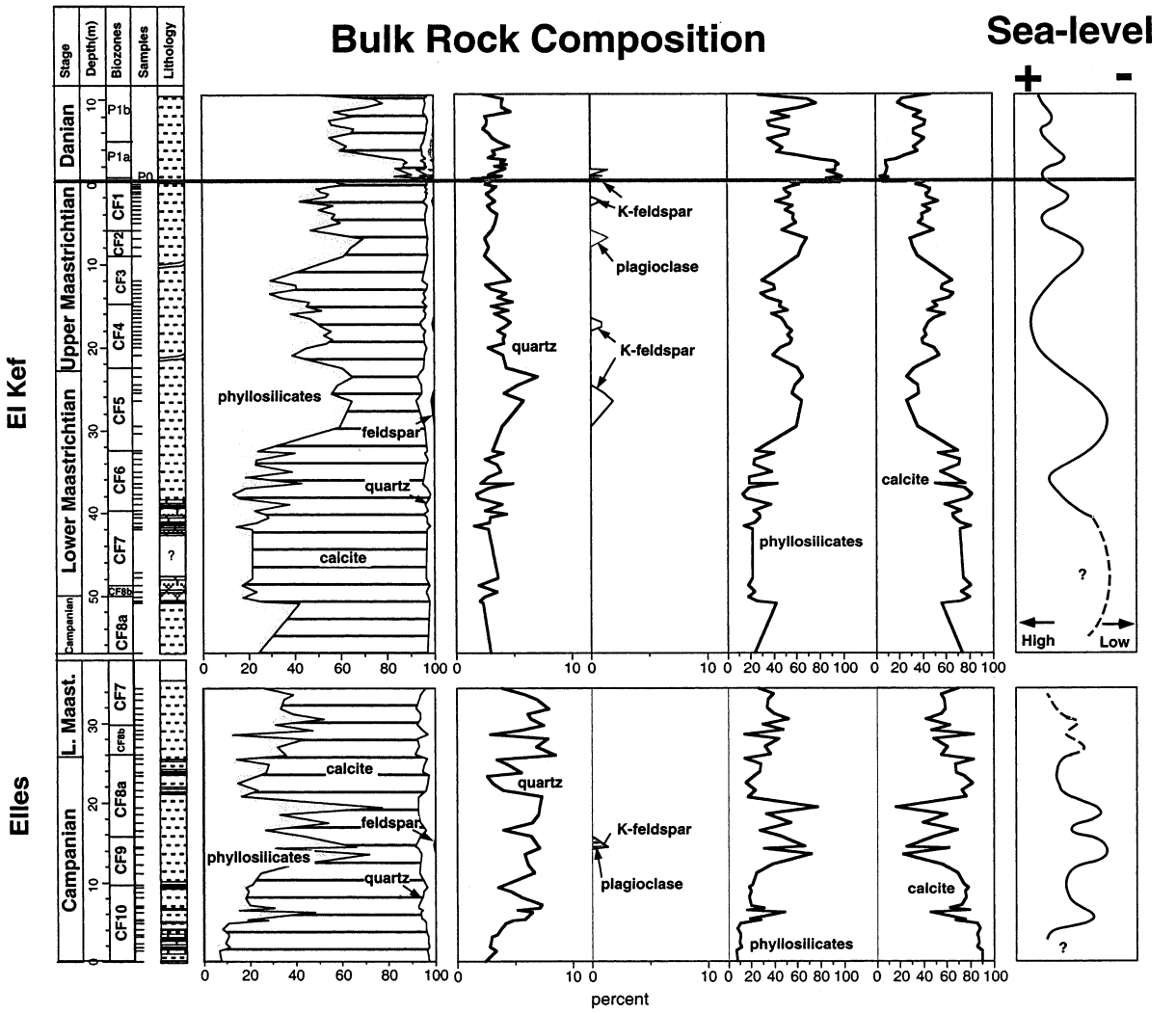

Fig. 10. Late Cretaceous to early Tertiary bulk rock compositions in a composite section based on Elles (upper Campanian to lower Maastrichtian Zone CF7) and El Kef (lower Maastrichtian Zone CF7 to Paleocene Zone Plc). Stippled and numbered intervals mark sea-level lowstands 1–8 identified based on biostratigraphic, sedimentological, mineralogical and geochemical proxies (Li et al., 1999, 2000; this study). Note that major peaks in phyllosilicates and quartz mark major sea-level lowstands. The long-term increase in phyllosilicates beginning in Zone CF5 culminates in the lower Danian Zones P0 and Pla and appears to be related to increased humidity, weathering and runoff from nearby terrestrial areas (e.g. Kasserine Island) and decreased productivity in the early Danian coupled with the extinction of the large tropical and subtropical planktic foraminiferal species near the K–T boundary.

biogenic material derived from surface waters of the ocean (Lindinger, 1988) and organic debris derived from adjacent continental regions, as observed in the upper Maastrichtian (Li et al., 2000). Rock-Eval analyses indicate that the organic matter is primarily of terrigenous origin (Type III, Li et al., 2000). The TOC enrichment is therefore likely due to concentration and/or preservation of continental organic matter during condensed sedimentation associated with a high sea-level (maximum flooding surface). Large-scale defoliation of terrestrial plants due to an impact (Orth et al., 1981; Tschudy and Tschudy, 1984; Saito et al., 1986; Lindinger, 1988) and wildfires (Wolbach et al., 1985) are unlikely in this region since no 'fern spike' or other major change is observed in palynoflora (Meon, 1990; Meon et al., 2002).

8. Campanian–Maastrichtian trends

Lower Maastrichtian and Campanian outcrop exposures are discontinuous at El Kef. For this reason this interval (CF10–CF7) was sampled at Elles and the lower Maastrichtian to Danian at El Kef (CF7–Plb). For lithological descriptions see Li et al., 1999, 2000). Here we present previously unpublished bulk rock and clay mineral compositions through this interval. Sediment accumulation rate averages are very low (0.5 cm/ka) for the upper Campanian–lower Maastrichtian interval as a result of hiatuses (see Li et al., 1999). For the upper Maastrichtian sediment accumulation rates average 2 cm/ka (Li and Keller, 1998a,b,c).

Bulk rock compositions at Elles and El Kef indicate cyclic variations in calcite and detrital minerals as well as a long-term trend of increasing phyllosilicates and decreasing calcite (Fig. 10). For example, the long-term trend in phyllosilicates from $<10\%$ in the late Campanian Zone CF10 reaches maximum values of 80–90% in Zone P0 and the lower part of the Zone P1a. During the same time, calcite decreases and quartz influx remains stable between 3 and 6%. This long-term trend in bulk rock compositions indicates a general increase in detrital influx beginning in the late Campanian and increasing through the Maastrichtian into the early Danian. This trend reflects a major regional change in weathering processes and hence climate. The overall increase in detrital influx correlates with the global cooling trend observed in oxygen isotope records from Sites 525 and 690 (Barrera, 1994; Li and Keller, 1998a, b).

Phyllosilicate/calcite fluctuations within this long-term trend also reflect sea-level changes with high detrital abundances generally associated with low sea-levels and high terrestrial influx (notably K-feldspar and quartz). Based on these proxies, seven major sea-level lowstands can be recognized between the late Campanian and Maastrichtian (stippled pattern, Fig. 10). An additional sea-level regression has been recognized near the top of Zone CF1 in this study as noted earlier (Fig. 5C). The seven sea-level fluctuations correlate well with those previously identified based on various geochemical (stable isotopes, Sr/Ca ratios, TOC) faunal (macro- and microfossils, trace fossils) and sedimentological (marl/limestone transitions, hardgrounds, hiatuses) proxies (Li et al., 1999, 2000). Low sea-levels are generally associated with increased terrigenous influx, low kaolinite/chlorite+mica ratios, high TOC and high Sr/Ca ratios, whereas high sea-levels are generally associated with the reverse conditions.

Clay mineral compositions also show short-term and long-term trends. Short-term variations are seen in cyclic patterns of kaolinite, chlorite and mica which suggest alternating humid/warm and seasonal/dry climates (Fig. 11). Long-term trends are reflected in the kaolinite and smectite abundances and represent the long-term cooling

Fig. 11. Late Cretaceous to early Tertiary clay mineral compositions in a composite section based on Elles (upper Campanian to lower Maastrichtian Zone CF7) and El Kef (lower Maastrichtian Zone CF7 to Paleocene Zone Plc). Stippled intervals mark sea-level lowstands. Note the absence of kaolinite in the upper Campanian Zone CF10, rapid increase in kaolinite in Zone CF9 and again in CF4, and near the K–T boundary. These increases in kaolinite mark a climate trend from arid/dry in the late Campanian to increasingly perennially wet and warm during the Maestrichtian–lower Paleocene interval, in the southwestern Tethys region.

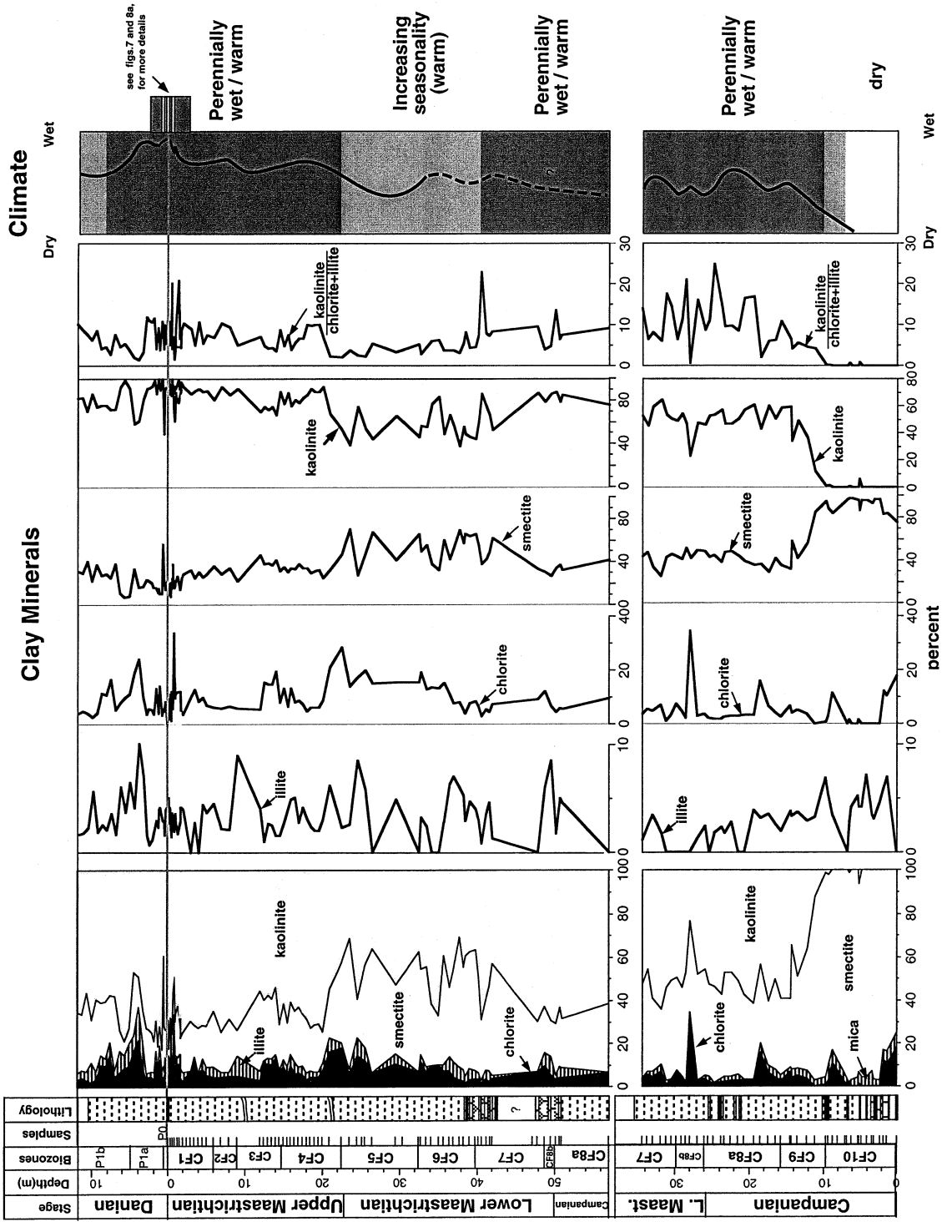
El Kef
Elles
Stage
Depth(m)
Biozones
Samples
Lithology
Danian
Lower Maastrichtian
Upper Maastrichtian
Campanian
L. Maast.
P1b
P1a
P0
CF1
CF2
CF3
CF4
CF5
CF6
CF7
CF8a
CF8b
CF9
CF10
Clay Minerals
kaolinite
chlorite+illite
illite
smectite
chlorite
mica
percent
Climate
Dry
Wet
see figs.7 and 8a, for more details
Perennially wet / warm
Increasing seasonality (warm)
dry

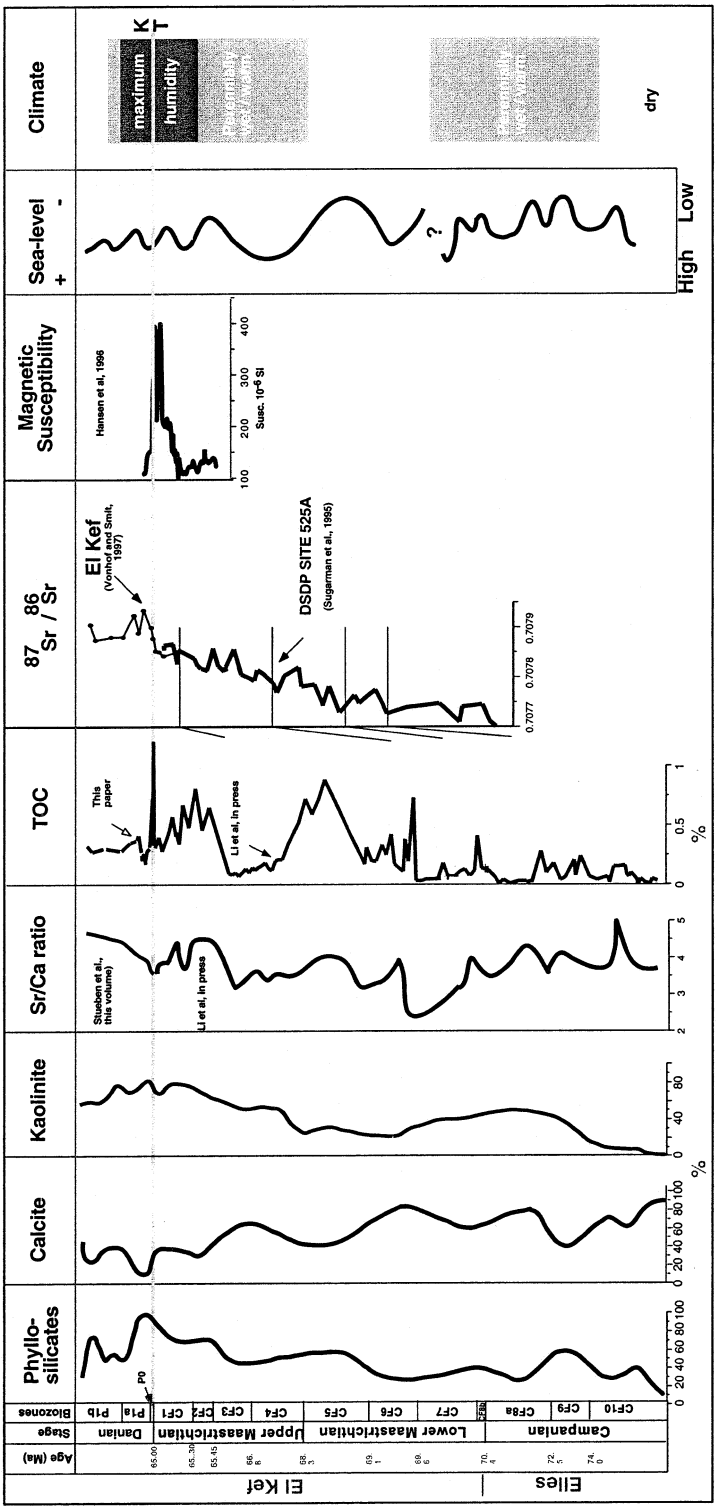
Climate
Sea-level + -
Magnetic Susceptibility
87 86 Sr / Sr
TOC
Sr/Ca ratio
Kaolinite
Calcite
Phyllo-silicates
Age (Ma)
Stage
Biozones
El Kef
Elles
Campanian
Lower Maastrichtian
Upper Maastrichtian
Danian
CF10
CF9
CF8a
CF8b
CF7
CF6
CF5
CF4
CF3
CF2
CF1
P1a
P1b
P0
K
T
maximum humidity
dry
High
Low
?
Hansen et al, 1996
Susc. 10-6 SI
El Kef
(Vonhof and Smit, 1997)
DSDP SITE 525A
(Sugerman et al., 1995)
This paper
Li et al, in press
Stueben et al., this volume)
%

trend with increased weathering. During the late Campanian (CF9–CF10), smectite dominates and kaolinite is nearly absent which suggests a seasonal to arid climate in this part of northern Africa. From CF8 upwards, kaolinite dominates with maximum abundance between the latest Maastrichtian (CF2–CF1) and early Danian (P1a). Smectite, chlorite and mica are present in variable abundances. This clay mineral pattern suggests that from the latest Campanian Zone CF8 through the Maastrichtian, Tunisia was characterized by humid (high precipitation) and warm climatic conditions, though with increased seasonality in the late early Maastrichtian (Zones CF6–CF5) as suggested by the kaolinite/chlorite+smectite ratio (Fig. 11).

The brief smectite maximum near the base of Pla at El Kef and Elles (Fig. 6) is anomalous in this trend and may be explained by sea-level fluctuations. Smectite consists of fine particles which are easily carried into slope and basin environments during transgressive seas, as was the case in the earliest Zone Pla. Coarser clay particles, such as kaolinite, chlorite and mica, are trapped in neritic environments (Adatte, 1987; Chamley, 1989; Weaver, 1989). During the late Maastrichtian (Zone CF4 upwards), the general clay mineral trend of increasing kaolinite appears to be linked to a regional climate change towards more humid, wet, though not necessarily warmer, climatic conditions with minor sea-level fluctuations. Middle and high latitude stable isotope records indicate that climate cooled significantly during the CF4–CF3 time interval (Barrera, 1994; Li and Keller, 1998a,b). Clay mineral data from Tunisia thus suggest that the late Maastrichtian was a time of increased humidity in the low latitude Tethys, coinciding with the cooling observed in high latitudes.

9. Other sea-level and climate proxies

Strontium concentrations in marine sediments have been successfully used to infer sea-level fluctuations (Graham et al., 1982; Renard, 1986; Stoll and Schrag, 1996). Sr/Ca ratios measured in well-preserved planktic foraminifera from the Elles and El Kef sections yield relatively accurate records of Sr fluctuations in seawater and consequently sea-level changes (Li et al., 2000). A strong correlation exists between variations of Sr/Ca ratios in planktic foraminifera with global sea-level fluctuations due to the shifts in sink and source of Sr during sea-level falls and rises. All major increases in Sr/Ca values coincide with sea-level lowstands (Fig. 12). But from CF5 upwards, the Sr/Ca record also shows an overall increase in the Sr/Ca ratio which may reflect a long-term change in the Sr due to the increased weathering rate indicated by bulk and clay mineralogy.

At El Kef and Elles, TOC values are generally high during low sea-levels either as a result of enhanced primary productivity, or more likely high terrestrial organic influx, as confirmed by Rock-Eval analyses (Li et al., 2000). From CF6–CF5 upwards, TOC values gradually increase with maxima occurring during sea-level lows. This overall TOC increase reflects increasing run-off due to intensified weathering on land under perennially wet climatic conditions (Fig. 12). A reverse trend is observed in the K–T clay layer where high TOC contents is associated with a sea-level rise.

Sr^{87}/Sr^{86} ratios are linked to weathering and erosion and indirectly to sea-level and climate changes. At DSDP Site 525 in the South Atlantic, Sr^{87}/Sr^{86} ratios show a continuous rise throughout the Maastrichtian with maximum values between 300 and 400 ka (CF2–CF1 transition) before the K–T boundary (Fig. 12) as also observed in other studies (Sugarman et al., 1995; Hess et al., 1986;

Fig. 12. Summary of late Cretaceous sea-level and climate fluctuations inferred from mineralogical proxies (phyllosilicates, calcite, kaolinite) and various geochemical proxies, including Sr/Ca ratios, Sr^{87}/Sr^{86} ratios, TOC, and magnetic susceptibility (Hansen et al., 1996). Stippled interval marks low sea-levels. Note that from the early late Maastrichtian onwards, the gradual increase in each of the proxies (except calcite) indicates a change in weathering rates due to increased humidity. Within this long-term change, the major sea-level regressions generally correlate with high Sr/Ca ratios, high TOC and high terrigenous influx.

Arthur et al., 1992; Frank and Arthur, 1999). Data from El Kef and Bidart (Vonhof and Smit, 1997) indicate a further increase in Sr^{87}/Sr^{86} ratios with a maximum at the P0–P1a transition (Fig. 12). A rise in Sr^{87}/Sr^{86} ratios reflects increased weathering due to enhanced rainfall. Intensive leaching of soils and sialic surface rocks located on the African craton likely contributed to the Sr runoff to the ocean. Within this long-term trend, Deccan Trap volcanism could have induced the 0.0004 decrease in Sr^{87}/Sr^{86} ratio observed in the middle part of Zone CF1 at El Kef (Vonhof and Smit, 1997; Martin and McDougall, 1991).

Magnetic susceptibility of sediments is linked to abundance of magnetic minerals and phyllosilicates (Hansen et al., 1996; Urrutia-Fucugauchi, 1997) and indirectly to enhanced continental runoff due to rainfall. Hansen et al. (1996) observed that magnetic susceptibility for the latest Maastrichtian at El Kef reached maximum values in the upper part of Zone CF1 (Fig. 12) as also observed at Elles by Hambach (personal communication, 1999). This magnetic susceptibility maximum correlates with the sea-level lowstand identified in this study in the upper Zone CF1 (Fig. 5A).

10. Discussion

Sea-level and climate proxies, such as bulk rock and clay mineral compositions, TOC Sr/Ca and Sr^{87}/Sr^{86} ratios, indicate that Maastrichtian sediments from the southwest Tethys initiate a gradual climatic change towards more humid, though not necessarily warmer, conditions. This change in weathering flux, including the increasing CO_2 consumption, significantly contributed to climate cooling by effecting an increased drawdown of atmospheric PCO_2. Within this long-term climate change, maximum humid conditions are reached just before the K–T boundary (top CF2 and CF1 Zones) and in the earliest Danian (P0 to basal P1a, Figs. 8B, 11). Eight sea-level lowstands are identified between the late Campanian and the K–T boundary with estimated ages and durations for the first seven given by Li et al. (1999, 2000) as: late Campanian ~74.2 Ma, 73.4–72.5 Ma and 72.2–71.7 Ma, early Maastrichtian 70.7–70.3 Ma, 69.6–69.3 Ma and 68.9–68.3 Ma, and late Maastrichtian 65.45 Ma. This study confirms these sea-level fluctuations based on bulk rock and clay mineral compositions and adds one additional brief sea-level lowstand in the latest Maastrichtian ~25–100 ka before the K–T boundary. Major eustatic sea-level falls identified by Haq et al. (1987) coincide with Tethyan sea-level falls identified at 68.9–68.3 Ma, 70.7–70.3 Ma and ~74.2 Ma. This suggests that these fluctuations are of eustatic origin. The late Maastrichtian sea-level low at 65.45 Ma is also likely of eustatic origin as indicated by its presence in sedimentological sequences worldwide (Keller and Stinnesbeck, 1996). A sea-level transgression marks the end of the Maastrichtian and maximum flooding coincides with the K–T boundary clay layer (e.g. Donovan et al., 1988; Baum and Vail, 1988; Keller and Stinnesbeck, 1996; Stinnesbeck et al., 1998). The early Danian sea-level falls near the P0–Pla and Pla–Plb boundaries have been identified worldwide (MacLeod and Keller, 199la,b; Keller and Stinnesbeck, 1996).

Stable isotope records from South Atlantic Sites 525 and 690C (Fig. 13, Barrera, 1994; Barrera et al., 1997; Li and Keller, 1998a) indicate that the cooling trend in sea surface waters began some time in the late Campanian (CF10) and reached maximum lows in Zones CF4–CF3 in the high latitude Site 690 and near the top of

Fig. 13. Summary of late Cretaceous to early Paleocene sea-level and climate fluctuations and the species richness in planktic foraminifera in Tunisia and correlation with the $\delta^{18}O$ record from the South Atlantic Site 525 (Li and Keller, 1998b). Note the early late Maastrichtian was a time of increased humidity in the southwestern Tethys and cooling in high latitudes. Species richness in planktic foraminifera correlates significantly with this gradual change in climate, weathering and nutrient import to the oceans. The pre-K–T boundary decrease in species richness in Zones CF1–CF2 (65.45 Ma) coincides with the onset of maximum humidity in Tunisia and a short warm event in the southern high latitudes.

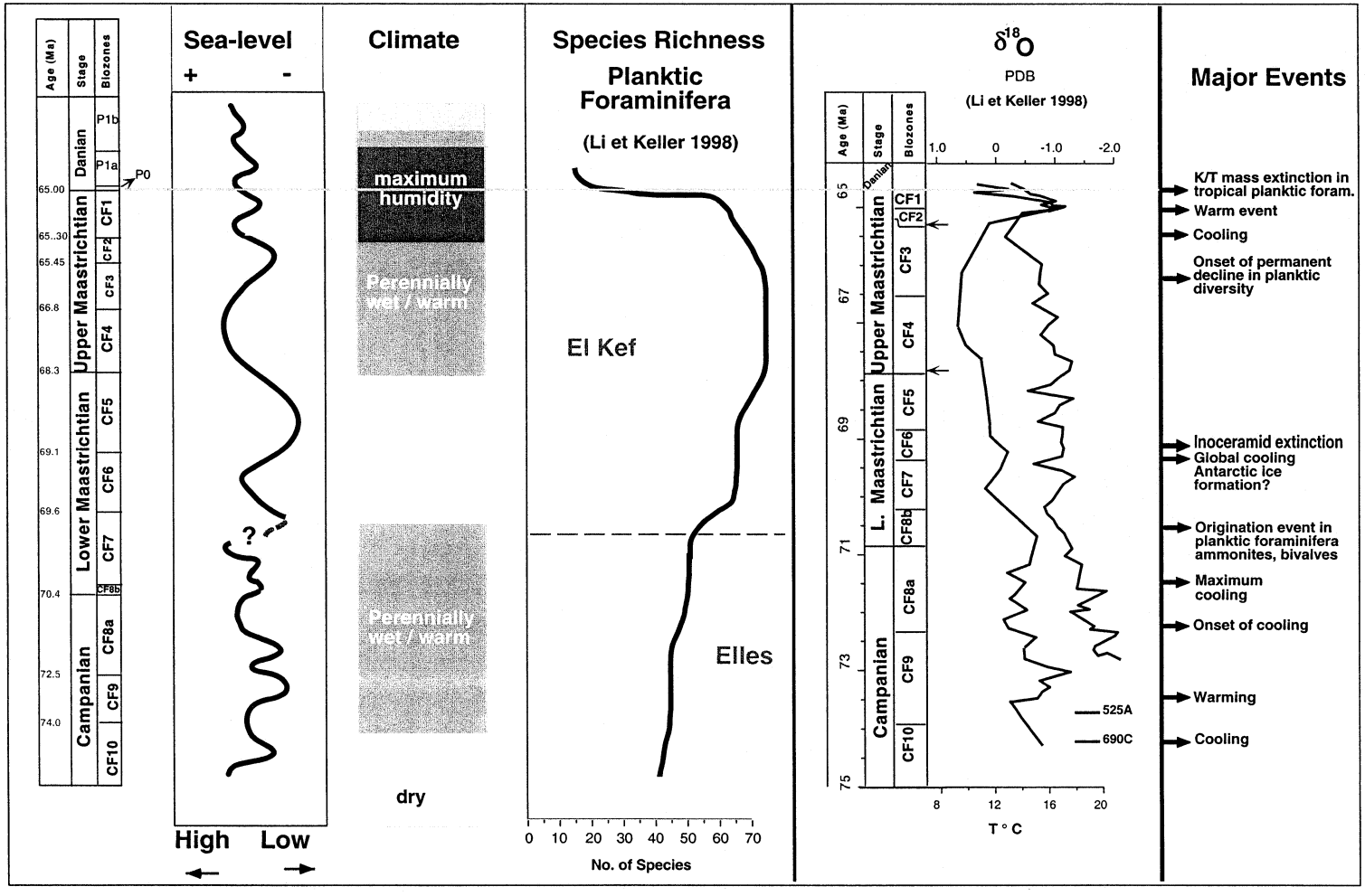
Tethys (Tunisia)
South Atlantic
Age (Ma)
Stage
Biozones
Danian
P1b
P1a
P0
Upper Maastrichtian
CF1
CF2
CF3
CF4
Lower Maastrichtian
CF5
CF6
CF7
CF8b
Campanian
CF8a
CF9
CF10
65.00
65..30
65.45
66.8
68.3
69.1
69.6
70.4
72.5
74.0
Sea-level
+
-
?
High
Low
Climate
maximum humidity
Perennially wet / warm
Perennially wet / warm
dry
Species Richness
Planktic Foraminifera
(Li et Keller 1998)
El Kef
Elles
0 10 20 30 40 50 60 70
No. of Species
δ18O
PDB
(Li et Keller 1998)
1.0 0 -1.0 -2.0
L. Maastrichtian
65
67
69
71
73
75
525A
690C
8 12 16 20
T° C
Major Events
K/T mass extinction in tropical planktic foram.
Warm event
Cooling
Onset of permanent decline in planktic diversity
Inoceramid extinction
Global cooling
Antarctic ice formation?
Origination event in planktic foraminifera ammonites, bivalves
Maximum cooling
Onset of cooling
Warming
Cooling

CF3–CF2 in the middle latitude Site 525 (Fig. 13). This cooling trend is interrupted by periodic warming in surface waters and the influx of warmer deep waters in middle latitudes in Zones CF5 and CF6. A major short-term warming marks the interval between 200 and 400 ka before the K–T boundary (Li and Keller, 1998a, b). These major cooling and warming phases generally coincide with sea-level fluctuations identified in the southwestern Tethys (Figs. 10, 12). Some authors suggest that the long-term Campanian–Maastrichtian cooling may have been due to polar ice in Antarctica (Barrera, 1994; Abreu et al., 1998). If this hypothesis can be confirmed, then the late Cretaceous sea-level changes observed in Tunisia may be related to high latitude cooling and possible ice caps on Antarctica.

Clay mineral data suggest that the high latitude cooling during the late Campanian and Maastrichtian was associated with increased humidity in the southwestern Tethys. This reflects climatic conditions that are similar to the last Quaternary glacial episode when the Sahara region experienced humid conditions and greened with abundant vegetation. Maximum humidity characterized the K–T boundary and may be linked to greenhouse effect induced by Deccan volcanism. At this time, humidity was not restricted to the Tethys, but reached well into the middle latitudes as indicated by data from the South Atlantic Site 525 that suggests perennially wet conditions (significant increase in kaolinite) during the CF2–CF1 interval (Adatte et al., in preparation).

These changes in climate and associated oceanic circulation appear to have significantly affected planktic foraminiferal species richness as well as species richness in palynofloras and most invertebrates, except for inoceramids and rudistids which went extinct. For example, species richness doubled for most of these groups in Zone CF6 (as exemplified in Fig. 13 for planktic foraminifera) following the first cooling maximum between 71 and 70 Ma and reached maximum richness in CF4 and CF3 (Keller and Li, in press). Note that the maximum species richness coincides with increasing calcite, high kaolinite and decreasing phyllosilicates in Zones CF4–CF3 (Figs. 10, 11). The terminal decline in species richness, which begins in Zone CF2 and culminates at the K–T boundary, correlates with maximum humidity (Fig. 13). The decline in species richness also correlates with increased terrestrial influx and consequently nutrients. Nutrient export to the ocean probably reached a maximum in the upper CF1 to lower Pla interval. Carbon isotopes indicate that surface productivity decreased globally during the early Danian and may have adversely affected the watermass stratification and nutrient balance which contributed to the low species diversity and slow recovery of marine plankton after the mass extinction.

11. Conclusions

(1) El Kef and Elles sections contain the most expanded and complete sedimentary records known to date and therefore are the appropriate global standard stratotype and point (GSSP) and additional GSSP sections respectively.

(2) Our observations based on biostratigraphical, lithological and mineralogical data indicate that the K–T transition is marked by a sea-level lowstand in the latest Maastrichtian about 25–100 ka below the K–T boundary. This sea-level fall is marked by increased detrital input at El Kef and Elles and a short hiatus at Ain Settara. A rising sea-level marks the end of the Maastrichtian and is expressed at Elles and El Kef by deposition of a foraminiferal packstone. A flooding surface marks the K–T boundary clay associated with condensed sedimentation and maximum influx of terrestrial organic matter. The P0–P1a transition is marked by a sea-level lowstand corresponding to a short hiatus at Ain Settara where the upper part of P0 is missing and a period of non-deposition and erosion marks the lower part of P1a. At Seldja, P0 and possibly the topmost part of CF1 is missing.

(3) All the identified clay minerals are known from normal deposition or pedogenic environments and exist in various amounts within the Cretaceous and Paleogene. Thus there are no mineralogical components that are unique or that could be related to an exotic event. Kaolinite increases from the late Maastrichtian into the early

Danian and indicates overall increased humidity. Smectite peaks just below the K–T boundary and near the base of Pla indicate a sea-level rise linked with drier climatic conditions. At both El Kef and Elles sections, the K/SM ratios in Zone P0 suggest a series of alternating warm humid and seasonal temperate climate (Fig. 7). Sea-level and climate fluctuations inferred from bulk rock and clay mineral data indicate a consistent relationship of low sea-levels with high humidity and high sea-levels with low humidity (increasing seasonality) in the southwestern Tethys region (Fig. 8B).

(4) Terrestrial organic matter, as well as Ir and other trace elements, are concentrated at the K–T boundary clay layer which globally coincides with a sea-level rise (maximum flooding) and implies sediment starvation and a condensed interval (Fig. 8B). These trace elements are therefore significantly elevated as a result of concentration and additional influx due to extraterrestrial event must be evaluated with respect to normal flux.

(5) Late Campanian to early Danian trends in bulk rock compositions indicate an increasing detrital influx that culminated during the K–T transition and reflect a global change in weathering and climate. At the same time, clay minerals indicate a long-term trend towards a more humid climate which also culminated during the K–T transition. For the same interval, middle and high southern latitude oxygen isotope records indicate long-term climate cooling. This suggests that during the Maastrichtian humidity increased in low latitudes whereas high latitudes cooled. The short-term warming just below the K–T boundary may be linked to Deccan volcanism and may have enhanced already humid conditions in the Tethys region and increased continental runoff.

(6) The species richness patterns of planktic foraminifera, invertebrates (except inoceramids and rudistids) and palynoflora correlate significantly with the observed changes in climate and weathering. Doubling of species richness between Zones CF6 and CF5, following a major cool event, may be related to increased humidity and precipitation and the resultant increase in terrigenous influx, including terrestrial organic matter. The decrease in species richness in CF2–CF1 and subsequent mass extinction of tropical and subtropical taxa coincides with maximum humidity and terrestrial nutrient export to the oceans which may have been associated with Deccan volcanism and a bolide impact.

12. Uncited references

Adatte et al., 1998, 2000; Alvarez et al., 1980; Berggren et al., 1995; Courtillot et al., 1986; Hallam, 1992; Hansen and Toft, 2002; Mc Arthur, 1994; McLean, 1985; Parsons and Takahashi, 1973; Said, 1978; Tschudy et al., 1984

Acknowledgements

We thank Dr. M. Bel Haj Ali, Director of the Tunisian Geological Survey, for hosting the 1998 International Workshop on the K–T boundary in Tunisia and for supporting the field excursion and Dr. Habib Bensalem for arranging logistical support and guidance for the field excursion which made collection of samples from Ain Settara and Elles possible for participants. We thanks Jose 'Derrick' Richard for the sample preparation for XRD analysis, Philip Steimann for conducting TOC analysis, Jerry Baum and Hervé Chamley for their constructive reviews. This study was supported by grants from NSF INT 95-04309, DFG grant Sti 128/4-1 and the Swiss National Fund No. 8220-028367.

References

Abramovich, S., Keller, G., 2002. Planktic foraminiferal population changes during the Late Maastrichtian at Elles, Tunisia. Palaeogeogr. Palaeoclimatol. Palaeoecol.

Abreu, V.S., Hardenbol, J., Haddad, G., Baum, G.R., Droxler, A.W., Vail, P.R., 1998. Sequence stratigraphy of the European basins. Soc. Econ. Paleontol. Mineral. Spec. Publ. 60, 75–80.

Adatte, T., Rumley, G., 1989. Sedimentology and mineralogy of Valanginian and Hauterivian in the stratotypic region (Jura mountains, Switzerland). In: Wiedmann, J. (Ed.), Cretaceous of the Western Tethys Proceedings 3rd International Cretaceous Symposium. Scheizerbart'sche Verlagsbuchandlhung, Stuttgart, pp. 329–351.

Adatte, T., Stinnesbeck, W., Keller, G., 1996. Lithostratigraphic and mineralogic correlations of near K–T boundary clastic sediments in northeastern Mexico: Implications for origin and nature of deposition. Geol. Soc. Am. Spec. Pap. 307, 211–226.

Adatte, T., Keller, G., Li, L., Stinnesbeck, W., Zaghbib-Turki, D., 1998. Climate and sea level fluctuations across the K-T boundary in Tunisia: Warm and humid conditions linked to the Deccan volcanism? In: International Workshop on Cretaceous-Tertiary Transition, Office National des Mines, Direction du Service Geologique, Tunis, Tunisie, 1998. Abstracts, pp. 7–10.

Adatte, T., Bolle, M.P., De Kaenel, E., Gawenda, P., Winkler, W., Von Salis, K., 2000. Climatic evolution from Paleocene to earliest Eocene inferred from clay-mineral: a transect from northern Spain (Zumaya) to southern (Spain, Tunisia) and southern-east Tethys margins (Israel, Negev). GFF Meet. Proc. Geol. Soc. Sweden 122, 7–8.

Adatte, T., Keller, G., Li, L., in preparation. Short uppermost Maastrichtian greenhouse episode linked to Deccan, Evidence from the high latitude South Atlantic (Site 525a).

Alvarez, L.W., Alvarez, W., Asaro, F., Michel, H.V., 1980. Extraterrestrial causes for the Cretaceous-Tertiary extinction. Science 208, 1095–1108.

Barrera, E., 1994. Global environmental changes preceding the Cretaceous-Tertiary boundary: Early-late Maastrichtian transition. Geology 22, 877–880.

Barrera, E., Huber, B.T., 1990. Evolution of Antarctic waters during the Maestrichtian:Foraminifera oxygen and carbon isotope Ratios, Leg 113. In: Barker, P.F., Kennett, J.P., et al. (Eds.), Proc. Ocean Drill. Prog. Sci. Res. 113, 813–827.

Barrera, E., Savin, S.M., Thomas, E., Jones, C.E., 1997. Evidence for thermohaline-circulation reversals controlled by sea-level change in the latest Cretaceous. Geology 25, 715–718.

Baum, G.R., Vail, P.R., 1988. Sequence stratigraphic concepts applied to Paleogene outcrops, Gulf and Atlantic basins. In: Wilgus, C.K., Posamentier, H., Ross, C.A., Kendall, C.G. (Eds.), Sea-Level Changes: An Integrated Approach. Soc. Econ. Paleontol. Mineral. Spec. Publ. vol. 42, pp. 309–327.

Berggren, W.A., Kent, D.V., Swisher, C.C., Aubry, M.P., 1995. A revised Cenozoic geochronology and chronostratigraphy. SEPM 54, 129–213.

Brinkhuis, H., Zachariasse, W.J., 1988. Dinoflagellate cysts, sea level changes and planktic foraminifera across the Cretaceous/Tertiary boundary at El Haria, northeast Tunisia. Mar. Micropaleontol. 13, 153–190.

Brinkhuis, H., Visscher, H., 1994. New evidence for terrestrial ecosystem collapse at the KT and Permian/Triassic. In: New Developments Regarding the KT Event and other Catastrophes in Earth History. LPI Contribution vol. 825, p. 17.

Brinkhuis, H., Bujak, J.P., Smit, J., Versteegh, G.J.M., Visscher, H., 1998. Dinoflagellate-based sea surface temperature reconstruction across the Creaceous-Tertiary boundary. Palaeogeogr. Palaeoclimatol. Palaeoecol. 141, 67–83.

Burollet, P.F., 1956. Contribution a l'Etude Stratigraphique de la Tunisie Centrale. Annales des Mines et de la Geologie, Tunis vol. 18, 388 pp.

Burollet, P.F., Oudin, J.L., 1980. Paléocène et Eocène en Tunisie, Pétroles et Phosphates. In: Géologie Comparée des Gisements de Phosphates et des Pétroles. Bur. Rech. Géol. Min. Doc. vol. 24, pp. 205–216.

Cande, S.C., Kent, D.V., 1995. Revised calibration of the geomagnetic polarity timescale for the Late Cretaceous and Cenozoic. J. Geophys. Res. 100, 6093–6095.

Canudo, J.I., Keller, G., Molina, E., 1991. Cretaceous/Tertiary extinction pattern and faunal turnover at Agost and Caravaca: S.E. Spain. Mar. Micropaleontol. 17, 319–341.

Chamley, H., 1989. Clay Sedimentology. Springer-Verlag, Berlin, 623 pp.

Chamley, H., Deconinck, J.F., Millot, G., 1990. Sur l'abondance des minéraux smectitiques dans les sédiments marins communs déposés lors des périodes de haut niveau marin du Jurassique au Paléogène. C. R. Acad. Sci. Paris 311, 1529–1536.

Chamley, H., 1997. Clay mineral sedimentation in the Ocean. In: Paquet, H., Clauer, N. (Eds.), Soils and Sediments Mineralogy and Geochemistry. Springer, Berlin, pp. 269–302.

Courtillot, V., Besse, J., Vandamme, D., Montignie, R., Jaeger, J.J., Cappeta, H., 1986. Deccan flood basalts at the Cretaceous/Tertiary boundary? Earth Planet. Sci. Lett. 80, 361–374.

Deconinck, J.F., 1992. Sédimentologie des argiles dans le Jurassique-Crétacé d'Europe occidentale et du Maroc. Mém. Habilit. Lille I, 266 pp.

Donovan, A.D., Baum, G.R., Blechschmidt, G.L., Loutit, T.S., Pflum, C.E., Vail, P.R., 1988. Sequence stratigraphic setting of the Cretaceous-Tertiary boundary in central Alabama. In: Wilgus, C.K., Posamentier, H., Ross, C.A., Kendall, C.G. (Eds.), Sea-Level Changes: An Integrated Approach. Soc. Econ. Paleontol. Mineral. Spec. Publ. vol. 42, pp. 299–307.

Dupuis, C., Steurbaut, E., Molina, E., Rauscher, R., Aschuler, M., Tribovillard, N.P., Arenillas, I., Arz, J.A., Robaszynski, F., Caron, M., Larque, P., (in press). Biotic evolution and events across the Cretaceous/Tertiary (K-T) boundary in the newly discovered Ain Settara section (Kalaat-Senan area, Central Tunisia). Palaeogeogr. Palaeoclimatol. Palaeoecol.

Ferrero, J., 1965. Dosage des principaux minéraux des roches par diffraction de Rayon X. Rapport C.F.P., Bordeaux, inédit.

Ferrero, J., 1966. Nouvelle méthode empirique pour le dosage des minéraux par diffraction R.X. Rapport C.F.P., Bordeaux, inédit.

Galeotti, S., Coccione, R., 2002. Changes in coiling direction of Cibicidoides pseudoacutus across the Cretaceous-Tertiary transition of Tunisia: paleoecological and biostratigraphic implications. Palaeogeogr. Palaeoclimatol. Palaeoecol.

Gaucher, G., 1981. Les Facteurs de la Pedogenèse. G. Lelotte, Dison, 730 pp.

Graham, D.W., Bender, M.L., Williams, D.F., Keigwin, L.D., Jr., 1982. Strontium-calcium ratios in Cenozoic planktic foraminifera. Geochim. Cosmochim. Acta 46, 1281–1292.

Hallam, A., 1992. Phanerozoic Sea-Level Changes. Columbia University Press, New York, 266 pp.

Hansen, H.J., Toft, P., Mohabey, D.M., Sarkar, A., 1996. Lameta age: Dating the main pulse of the Deccan traps volcanism. Gondwana Geol. Mag. Nagpur India Spec. vol. 2, 365–374.

Hansen, H.J., Toft, P., 2002. Magnetic susceptibility and Ni-rich spinels at the K-T boundary in El Kef, Elles and Ain Settara, Tunisia. Palaeogeogr. Palaeoclimatol. Palaeoecol.

Haq, B.U., Hardenbol, J., Vail, P.R., 1987. Chronology of fluctuating sea levels since the Triassic. Science 235, 1156–1167.

Hess, J., Bender, M.l., Schilling, J.G., 1986. Evolution of the ratio of strontium 87 to strontium 86 in sea water from Cretaceous to present. Science 231, 979–984.

Karoui-Yakoub, N., Zaghbib-Turki, N., Keller, G., 2002. The Cretaceous-Tertiary (K-T) mass extinction in planktic foraminifera at Elles I and El Melah, Tunisia. Palaeogeogr. Palaeoclimatol. Palaeoecol.

Kaiho, K. et al., 1999. Oceanic primary productivity and dissolved oxygen levels at the Cretaceous-tertiary boundary: their decrease, subsequent warming and recovery. Paleoceanography 14, 511–524.

Keller, G., 1988a. Biotic turnover in benthic foraminifera across the Cretaceous/Tertiary boundary at El Kef, Tunisia. Palaeogeogr. Palaeoclimatol. Palaeoecol. 66, 153–171.

Keller, G., 1988b. Extinction, survivorship and evolution of planktic foraminifera across the Cretaceous/Tertiary boundary at El Kef, Tunisia. Mar. Micropaleontol. 13, 239–263.

Keller, G., 1993. The Cretaceous-Tertiary transition in the Antarctic Ocean and its global implications. Mar. Micropaleontol. 21, 1–45.

Keller, G., Benjamini, C., 1991. Paleoenvironment of the eastern Tehys in the early Paleocene. Palaios 6, 439–464.

Keller, G., Barrera, E., Schmitz, B., Mattson, E., 1993. Gradual mass extinction, species survivorship and long-term environmental changes across the Cretaceous/Tertiary boundary in high latitudes. Geol. Soc. Am. Bull. 105, 979–997.

Keller, G., Li, L., MacLeod, N., 1995. The Cretaceous/Tertiary boundary stratotype section at El Kef, Tunisia: How catastrophic was the mass extinction? Palaeogeogr. Palaeoclimatol. Palaeoecol. 119, 221–254.

Keller, G., Li, L., in press. Evidence for progressive mass extinction and onset 500 k.y. before the the K-T boundary. Dinofest 2000.

Keller, G., Stinnesbeck, W., 1996. Sea-level changes, clastic deposits, and megatsunamis across the Cretaceous-Tertiary boundary. In: MacLeod, N., Keller, G. (Eds.), Cretaceous/Tertiary Boundary Mass Extinction: Biotic and Environmental Changes. W.W. Norton, New York, pp. 415–450.

Keller, G., Adatte, T., Stinnesbeck, W., Stuben, D., Kramar, U., Berner, Z., Li, L., Perch- Nielsen, K., 1998. The Cretaceous-Tertiary transition on the shallow Saharan platform of southern Tunisa. Geobios 30, 951–975.

Keller, G., Adatte, T., Stinnesbeck, W., Luciani, V., Karoui, N., Zaghbib-Turki, D., 2002. Paleobiogeography of the Cretaceous-Tertiary mass extinction in planktic foraminifera. Palaeogeogr. Palaeoclimatol. Palaeoecol.

Klug, H.P., Alexander, L., 1974. X-ray Diffraction Procedures for Polycrystalline and Amorphous Materials, 1st, 2nd edn. Wiley, New York.

Kübler, B., 1983. Dosage quantitatif des minéraux majeurs des roches sédimentaires par diffraction X. Cahier de l'Institut de Géologie de Neuchâtel, Sér. AX Nos. 1.1 and 1.2.

Kübler, B., 1987. Cristallinite de l'illite, methods normalisees de preparations, methods normalisees de measures. Cahiers Institut of Geologie, Neuchatel, Ser. ADX 1, 13 pp.

Li, L., Keller, G., 1998a. Maastrichtian climate, productivity and faunal turnovers in planktic foraminifera in south Atlantic DSDP Site 525A and 21. Mar. Micropaleontol. 33, 55–86.

Li, L., Keller, G., 1998b. Abrupt deep-sea warming at the end of the Cretaceous. Geology 26, 995–998.

Li, L., Keller, G., 1998c. Diversification and extinction in Campanian-Maastrichtian planktic foraminifera of Northwestern Tunisia. Eclogae Geol. Helv. 91, 75–102.

Li, L., Keller, G., Stinnesbeck, W., 1999. The late Campanian and Maastrichtian in northwestern Tunisia: palaeoenvironmental inferences from lithology, macrofauna and benthic foraminifera. Cretac. Res. 20, 231–252.

Li, L., Keller, G., Adatte, T., Stinnesbeck, W., 2000. Late Cretaceous sea level changes in Tunisia: A multi-disciplinary approach. Geol. Soc. Lond. 157, 447–458.

Lindinger, M., 1988. The Cretaceous/tertiary boundary at El Kef and Caravaca: Sedimentological, geochemical and clay mineralogical aspects. PhD thesis, ETH, Zurich, 253 pp.

Loutit, T.S., Hardenbohl, J., Vail, P.R., Baum, G., 1988. Condensed sections: the key to age determination and correlation of continental margin sequences. In: Wilgus, C.K., Posamentier, H., Ross, C.A., Kendall, C.G. (Eds.), Sea-Level Changes: An Integrated Approach. Soc. Econ. Paleontol. Mineral. Spec. Publ. vol. 42, pp. 183–213.

Luciana, V., 2002. High-resolution planktonic foraminiferal analysis from the Cretaceous/Tertiary boundary at Ain Settara (Tunisia): evidence of an extended mass extinction. Palaeogeogr. Palaeoclimatol. Palaeoecol.

MacLeod, N., Keller, G., 1991a. Hiatus distribution and mass extinction at the Cretaceous/Tertiary boundary. Geology 19, 497–501.

MacLeod, N., Keller, G., 1991b. How complete are Cretaceous/Tertiary boundary sections? A chronostratigraphic estimate based on graphic correlation. Geol. Soc. Am. Bull. 103, 1439–1457.

Martin, E.E., Macdougal, J.D., 1991. Seawater Sr isotopes at the Cretaceous-Tertiary boundary. Earth Planet. Sci. Lett. 104, 166–180.

Mc Arthur, J.M., 1994. Recent trends in strontium isotope stratigraphy. Terra Nova 6, 331–358.

McLean, D.M., 1985. Deccan Traps mantle degassing in the terminal Cretaceous marine extinctions. Cretac. Res. 6, 235–239.

Meon, H., 1990. Palynologic studies of the Cretaceous/Tertiary boundary interval at El Kef outcrop, northwestern Tunisia:

Paleogeographic implication. Rev. Paleobot. Palynol. 65, 85–94.

Meon, H., Mannai, Armand, A., Desvignes, P., 2002. The K-T boundary in El Kef section and some other sites (Tunisia): evolution of the continental vegetation. Palaeogeogr. Palaeoclimatol. Palaeoecol.

Monaco, A., Mear, Y., Murat, A., Fernandez, J.M., 1982. Critères mineralogiques pour la reconnaissance des turbidites fines. C. R. Acad. Sci. Paris 295II, 43–46.

Moore, D., Reynolds, R., 1989. X-Ray-Diffraction and the Identification and Analysis of Clay-Minerals. Oxford University Press, Oxford, 332 pp.

Orth, C.J., Gilmore, J.S., Knight, J.D., Pillmore, C.L., Tschudt, R.H., Fasset, J.E., 1981. An iridium abundance anomaly at the palynological Cretaceous-Tertiary boundary in northern New Mexico. Science 214, 1314–1343.

Parsons, T.R., Takahashi, M., 1973. Biological Oceanographic Processes. Pergamon Press, Oxford, 186 pp.

Pospichal, J.J., 1994. Calcareous nannofossils at the K-T boundary; El Kef; no evidence for stepwise, gradual, or sequential extinctions. Geology 22, 99–102.

Remane, J., Keller, G., Hardenbohl, J., Ben Haj Ali, M., 1999. International workshop on Cretaceous-Paleogene transitions in Tunisia: The El Kef stratotype for the Cretaceous-Paleogene boundary reconfirmed. Episodes 22, 47–48.

Renard, M., 1986. Pelagic carbonate chemostratigraphy (Sr, Mg, $\delta^{18}O\delta^{13}C$). Mar. Micropaleontol. 10, 117–164.

Robaszynski, F., Gale, A., Juignet, P., Amedro, F., Hardenbohl, J., 1998. Sequence stratigraphy in the upper Cretaceous of the Anglo-Paris Basin: Exemplified by the Cenomanian stage. In: Mesozoic and Cenozoic Sequence Stratigraphy of European Basins, SEPM Spec. Publ. vol. 60, pp. 364–386.

Robert, C., Chamley, H., 1991. Development of early Eocene warm climates as inferred from clay mineral variations in oceanic sediments. Glob. Planet. Change 89, 315–332.

Robert, C., Kennett, J.P., 1992. Paleocene and Eocene kaolinite distribution in the South Atlantic and Southern Ocean Antarctic climate and paleoceanographic implications. Mar. Geol. 103, 99–110.

Said, R., 1978. Etude stratigraphique et micropaléontologique du passage Crétacé-Tertiaire du synclinal d'Elles (Région Siliana-Sers) Tunisie Centrale. Thèse 3ième Cycle, Université Pierre et Marie Curie, Paris IV, 275 pp.

Tschudy, R.H., Pillmore, C.L., Orth, C.J., Gilmore, J.S., Knight, J.D., 1984. Disruption of the terrestrial plant ecosystem at the Cretaceous-Tertiary boundary, Western Interior. Science 225, 1030–1032.

Saito, T., Yamanoi, T., Kaiho, K., 1986. End-Cretaceous devastation of terrestrial flora in the boreal Far east. Nature 323, 253–255.

Sassi, M., 1974. La sédimentation phosphatée au Paléocène dans le sud et le centre ouest de la Tunisie. These Sci., Orsay, 292 pp.

Schmitz, B., Keller, G., Stenvall, O., 1992. Stable isotope and foraminiferal changes across the Cretaceous/Tertiary boundary at Stevns Klint, Denmark: Arguments for long-term oceanic instability before and after bolide impact. Palaeogeogr. Palaeoclimatol. Palaeoecol. 96, 233–260.

Speijer, R.P., 1994. Extinction and recovery patterns in benthic foraminiferal paleocommunities across the Cretaceous/Paleogene and the Paleogene/Eocene boundaries. Geol. Ultraiectina vol. 124, 191 pp.

Stoll, H.M., Schrag, D.P., 1996. Evidence for glacial control of rapid sea level changes in the early Cretaceous. Science 272, 1771–1774.

Stinnesbeck, W., Keller, G., Adatte, T., Lopez-Oliva, J.G., MacLeod, N., 1996. Cretaceous-Tertiary boundary clastic deposits in Northeastern Mexico: Impact Tsunami or sea-level lowstand. In: MacLeod, N., Keller, G. (Eds.), Cretaceous/Tertiary Boundary Mass Extinction: Biotic and Environmental Changes. W.W. Norton, New York, pp. 471–517.

Urrutia-Fucugauchi, J., Ortega-Ramirez, J., Cruz Gatica, R., 1997. Rock-magnetic study of late Pleistocene-Holocene sediments from the Babícora lacustrine basin, Chihuahua, northern Mexico. Geofis. Int. 36, 23–47.

Vincent, S.J., Macdonald, D.I.M., Gutterridge, P., 1998. Sequence stratigraphy. In: Doyle, P., Bennet, M.R. (Eds.), Unlocking the Stratigraphical Record: Advances in Modern Stratigraphy.

Vonhof, H.B., Smit, J., 1997. High resolution late Maastrichtian-early danian oceanic 87Sr/86Sr record: implications for Cretaceous-tertiary boundary events. Geology 25, 347–350.

Weaver, C.E., 1989. Clays, muds and shales. In: Development in Sedimentology vol. 44. Elsevier, Amsterdam, 819 pp.

Wolbach, W.S., Lewis, R.S., Anders, E., 1985. Cretaceous extinctions: evidence for wildfires and search for meteoritic material. Science 230, 167–170.